Supplementary information

Oxygen-defective ruthenium oxide as an efficient and durable electrocatalyst for acidic oxygen evolution reaction

Jingwei Wang,†[a,b] Lejuan Cai,†[a] Zhipeng Yu,*[a,] Hao Tan,[a] Xinyi Xiang,[a] Kaiyang Xu,[a] Yang Chao,[a] Sitaramanjaneya Mouli Thalluri,[c] Fei Lin,[a] Haoliang Huang,[a] Chenyue Zhang,[a] Yang Zhao,[a] Wenlong Wang,*[a,b] and Lifeng Liu,*[a]

[a] Songshan Lake Materials Laboratory (SLAB), Dongguan 523808, P.R. China

[b] Institute of Physics, Chinese Academy of Sciences, Beijing 100090, P. R. China

[c] International Iberian Nanotechnology Laboratory (INL), 4715-330 Braga, Portugal

† J.W.W. and L.J.C. contributed equally to this work.

* To whom correspondence should be made.

E-mail: zhipeng.yu@inl.int (Z. P. Yu); wwl@iphy.ac.cn (W. L. Wang); liu.lifeng@sslab.org.cn (L. Liu)

Supplementary Figures

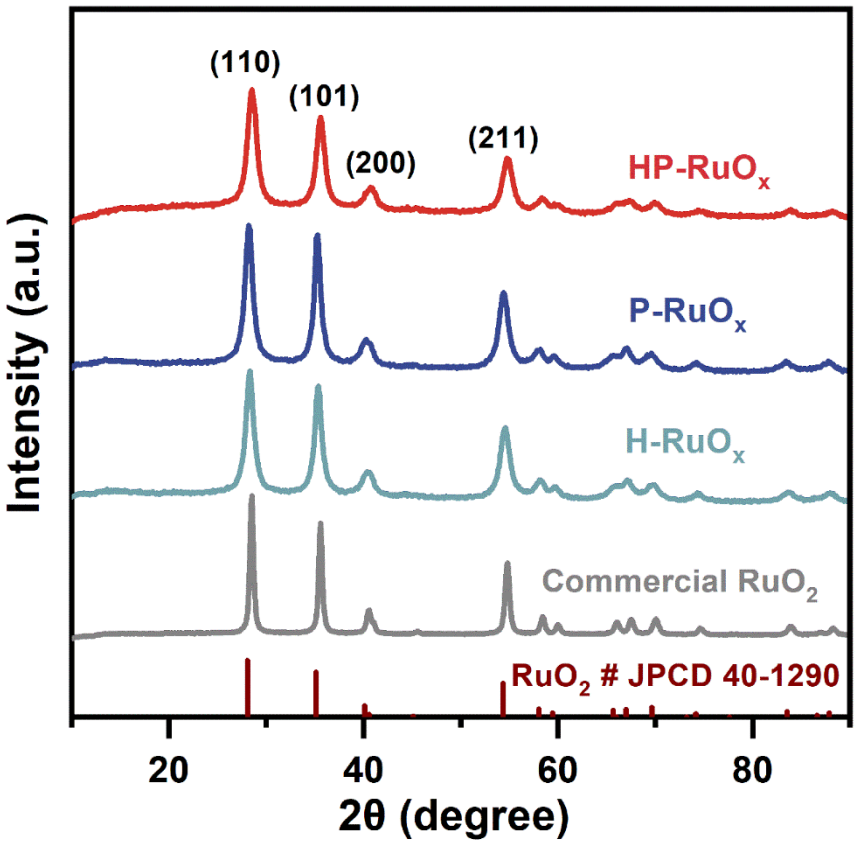

Fig. S1 XRD patterns of HP-RuO_x, P-RuO_x, H-RuO_x and commercial RuO_2. For reference, the standard diffraction patterns of rutile RuO_2 (JCPD No. 40-1290) is also presented.

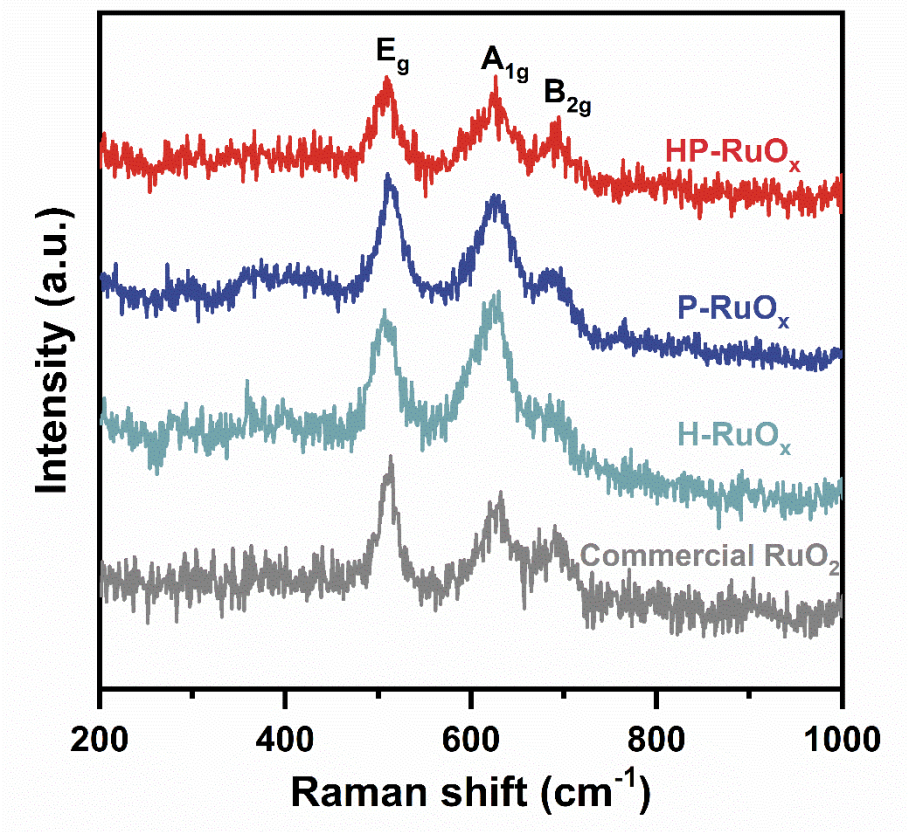

Fig. S2 Raman spectra of HP-RuO_x, P-RuO_x, H-RuO_x and commercial RuO_2.

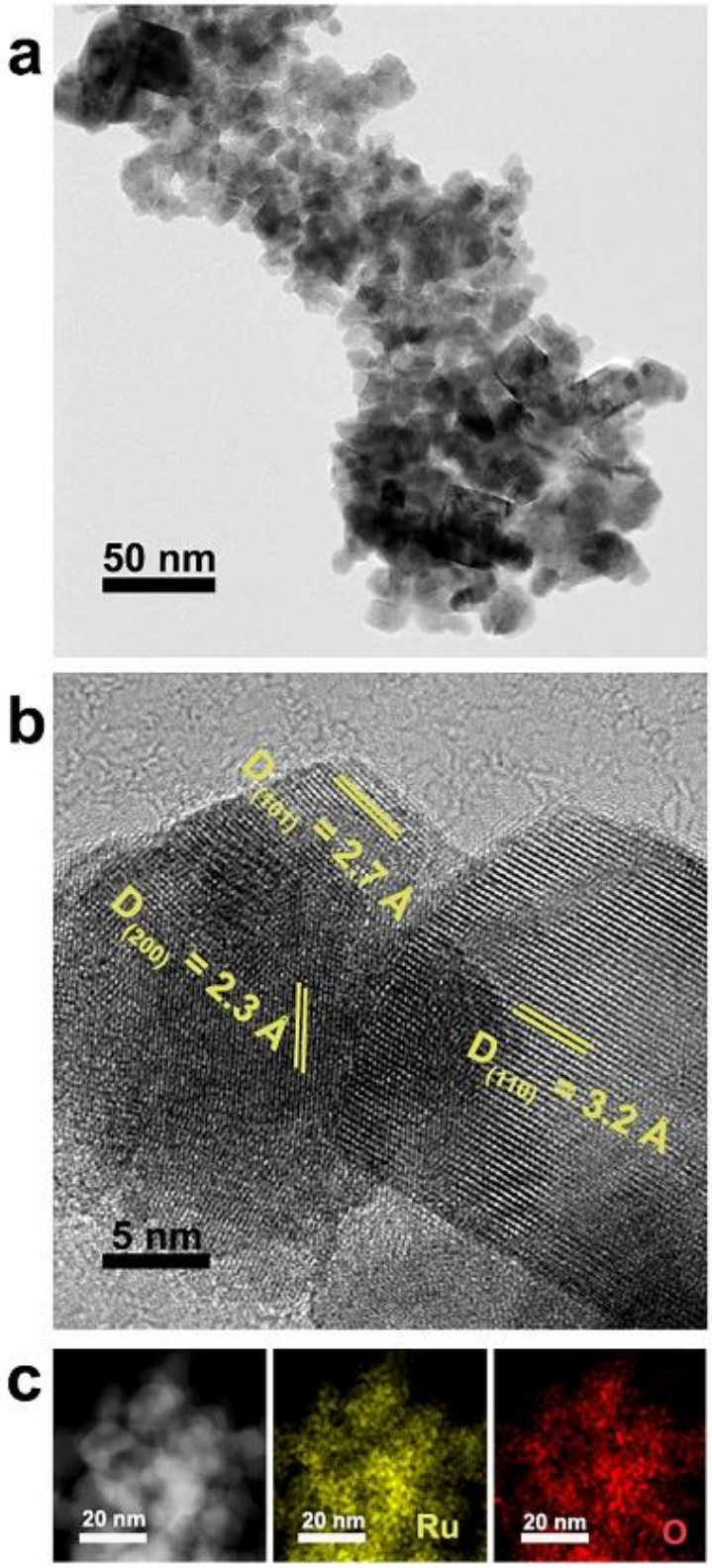

Fig. S3 (a) TEM image, (b) HRTEM image, (c) HAAF-STEM-EDS elemental maps of Ru and O for P-RuO_x.

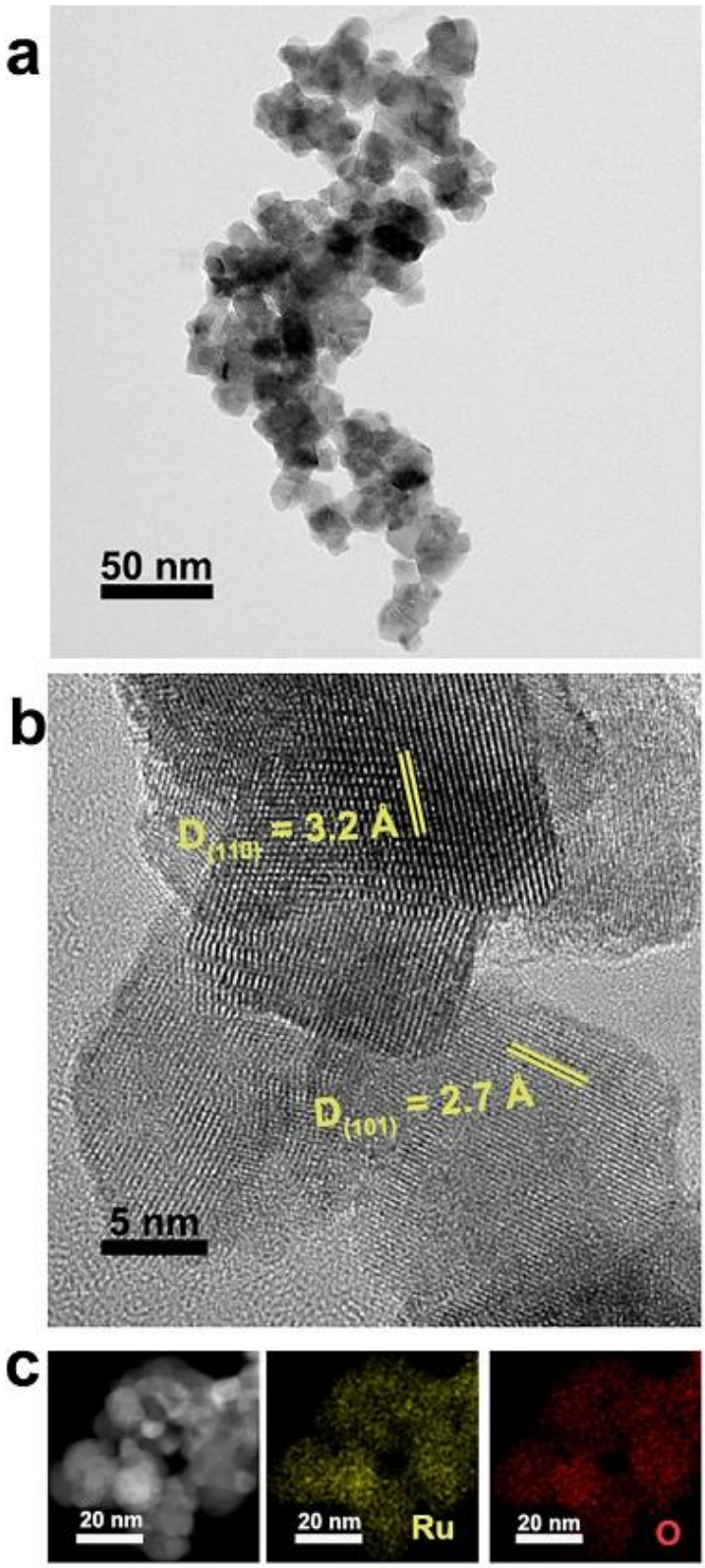

Fig. S4 (a) TEM image, (b) HRTEM image, (c) HAAF-STEM-EDS elemental maps of Ru and O for H-RuO_x.

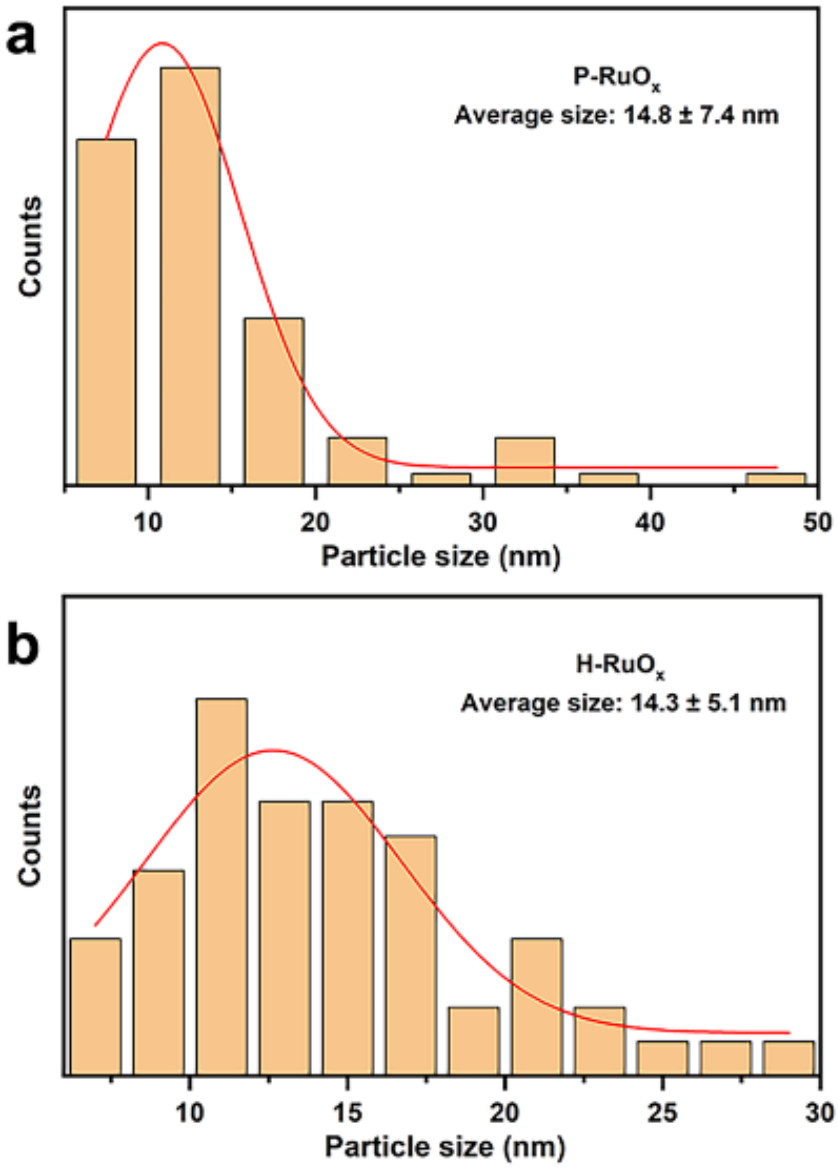

Fig. S5 Nanoparticle size distribution of (a) P-RuO_x and (b) H-RuO_x.

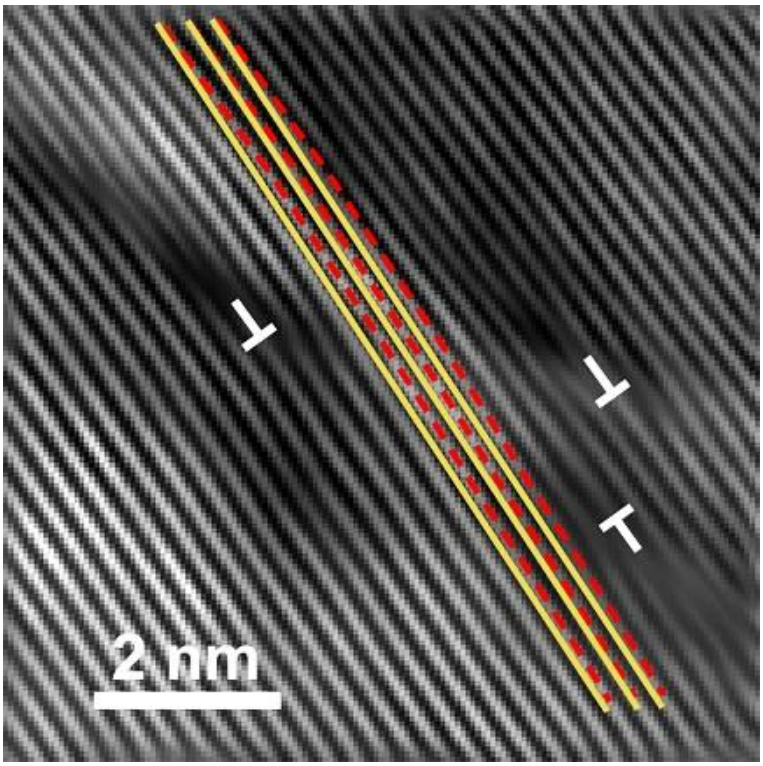

Fig. S6 Inverse fast Fourier transform (IFFT) pattern of **Fig. 1f**. The yellow solid and red dashed lines denote the ideal and actual lattice alignment orientations, respectively. The deviation between ideal and actual situations indicates lattice distortion in HP-RuO_x, while the white T-shaped marks represent lattice dislocations.

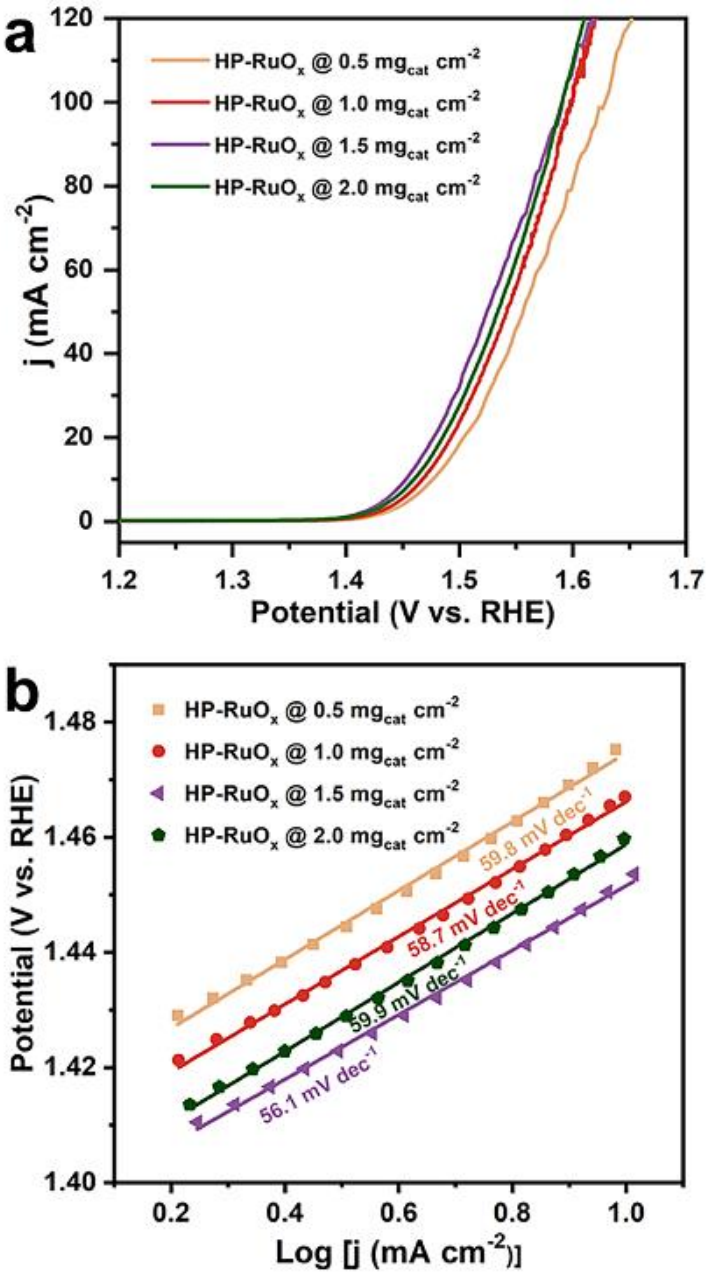

Fig. S7 (a) OER polarization curves and (b) corresponding Tafel slopes of HP-RuO$_x$ at different mass loadings.

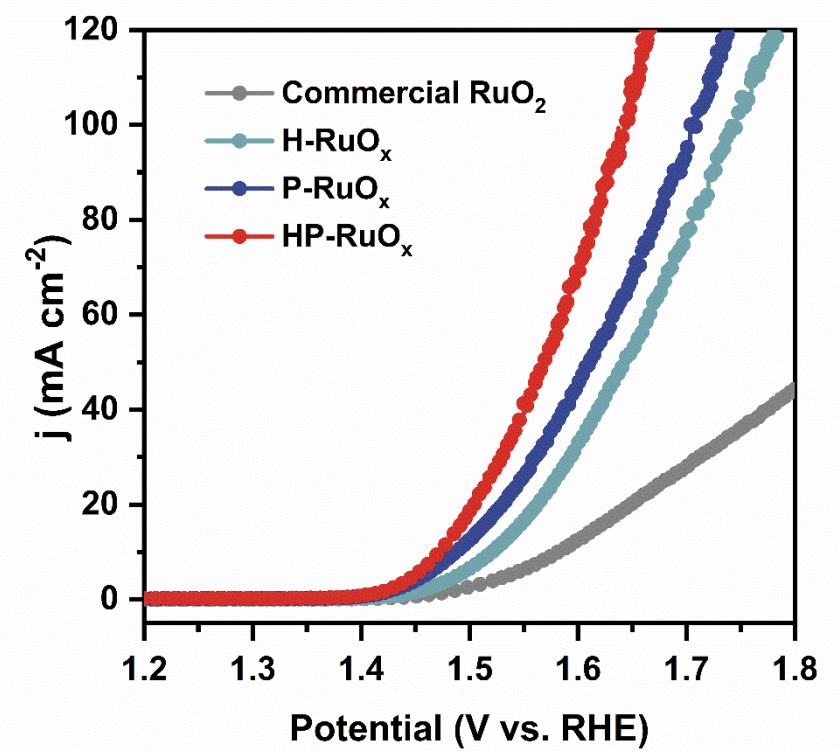

Fig. S8 OER polarization curves for different catalysts loaded on the Ti@Au felt recorded in 0.05 M H_2SO_4. The overpotentials (η_{10}) needed to deliver 10 mA cm^{-2} for HP-RuO_x, P-RuO_x, H-RuO_x and commercial RuO_2 are 243, 258, 291 and 352 mV, respectively. The loading density is 1 mg cm^{-2} for all catalysts.

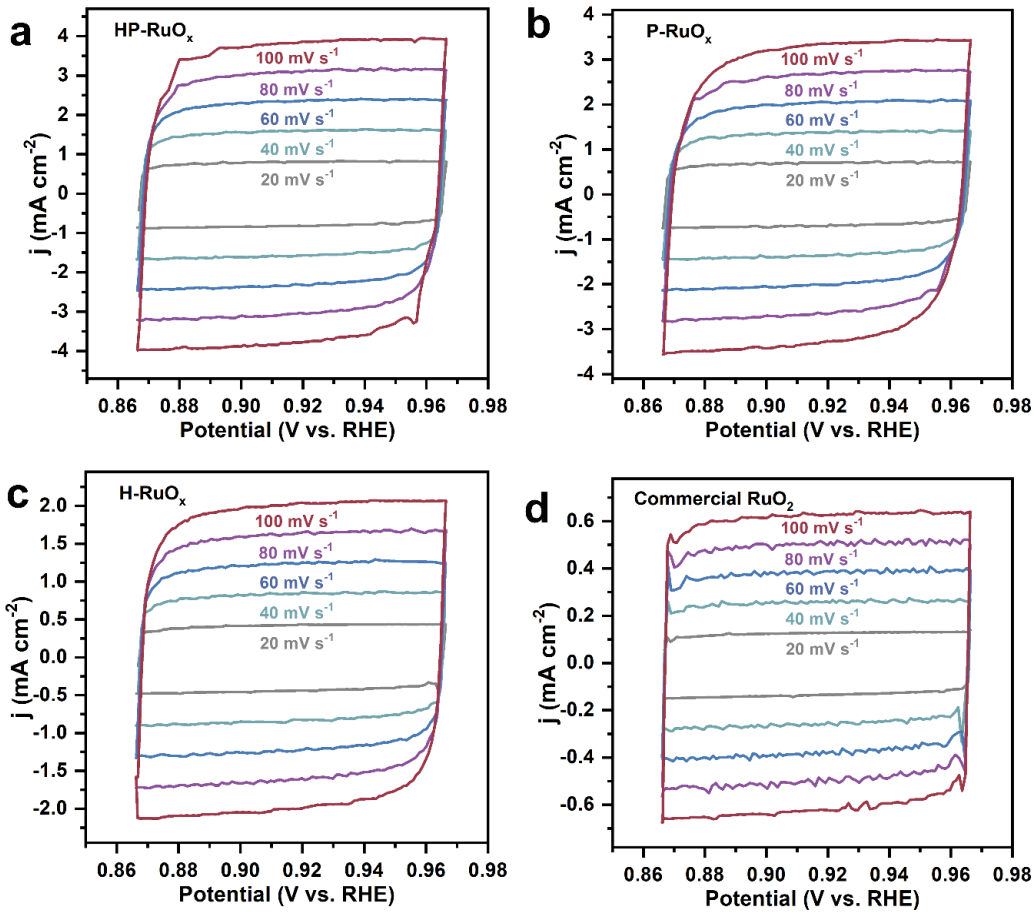

Fig. S9 Cyclic voltammograms recorded for (a) HP-RuO_x, (b) P-RuO_x, (c) H-RuO_x and (d) commercial RuO_2 in the potential region of 0.85 – 0.95 V vs. RHE at scan rates from 20 to 100 mV s^{-1}.

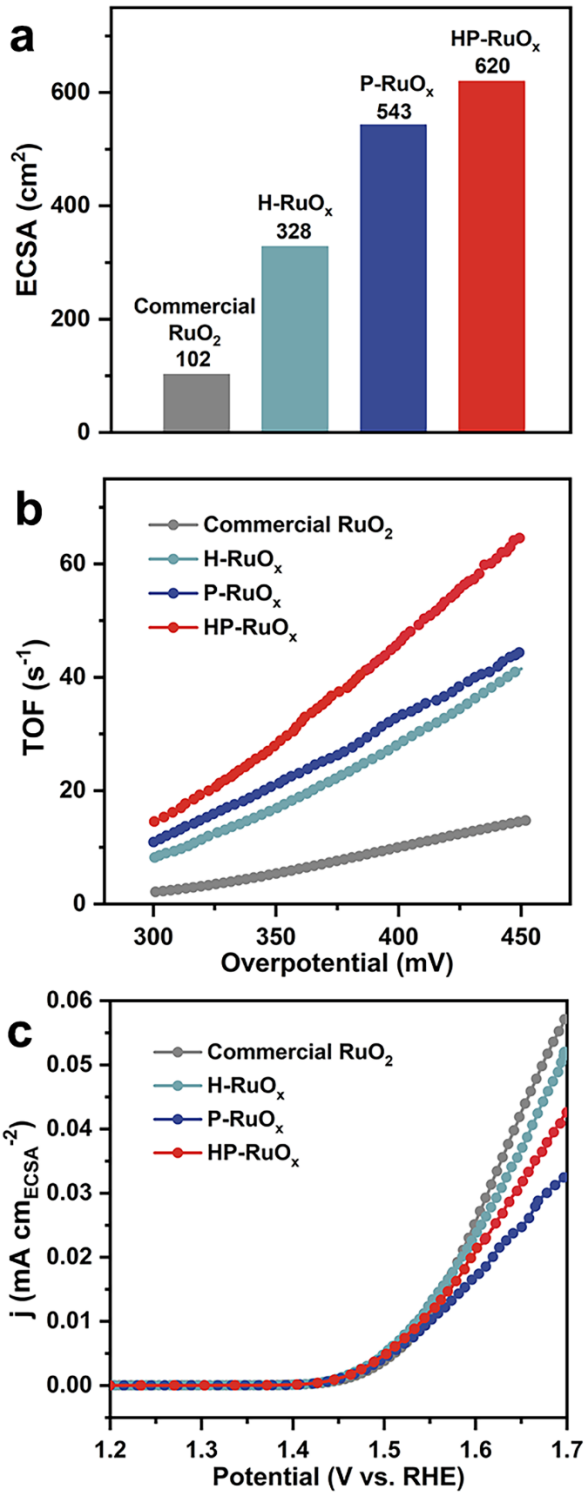

Fig. S10 (a) ECSA values, (b) ECSA normalized specific activity and (c) TOF at the overpotential of 300 − 450 mV of HP-RuO_x, P-RuO_x, H-RuO_x, and commercial RuO_2.

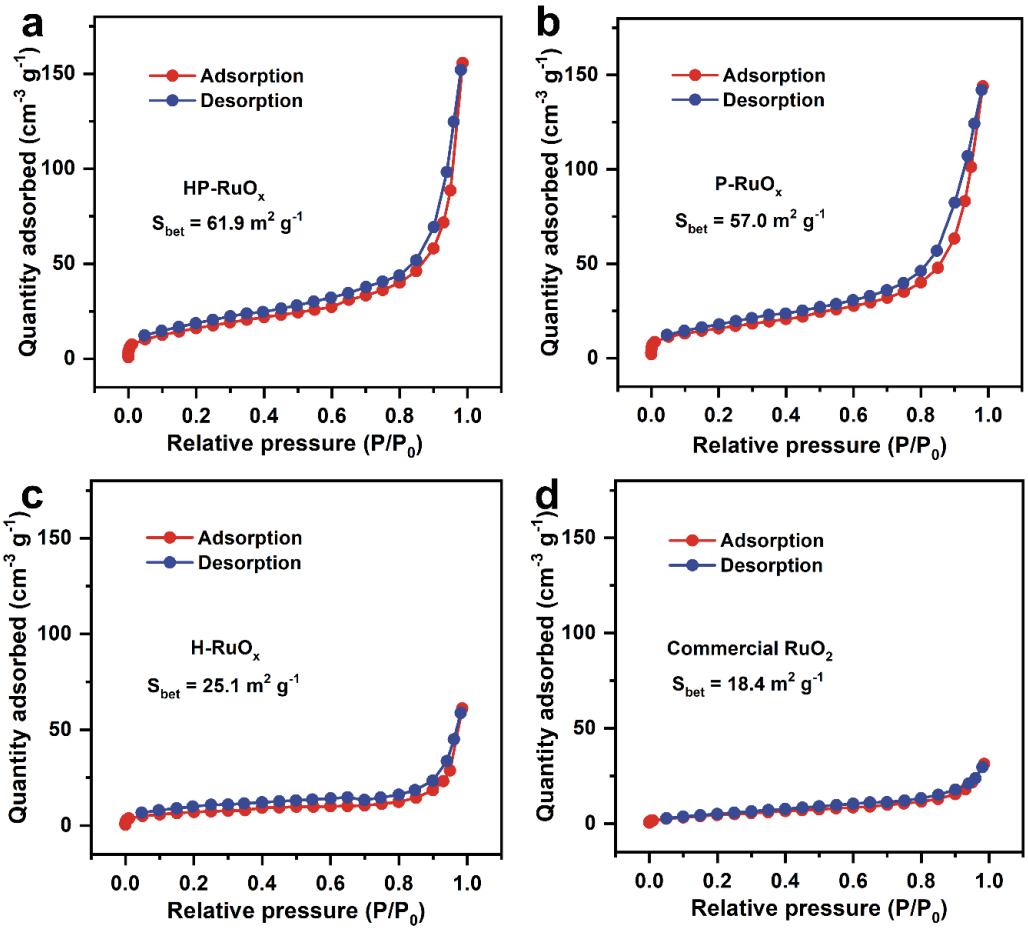

Fig. S11 N_2 adsorption/desorption isotherms of (a) HP-RuO_x, (b) P-RuO_x, (c) H-RuO_x, and (d) commercial RuO_2.

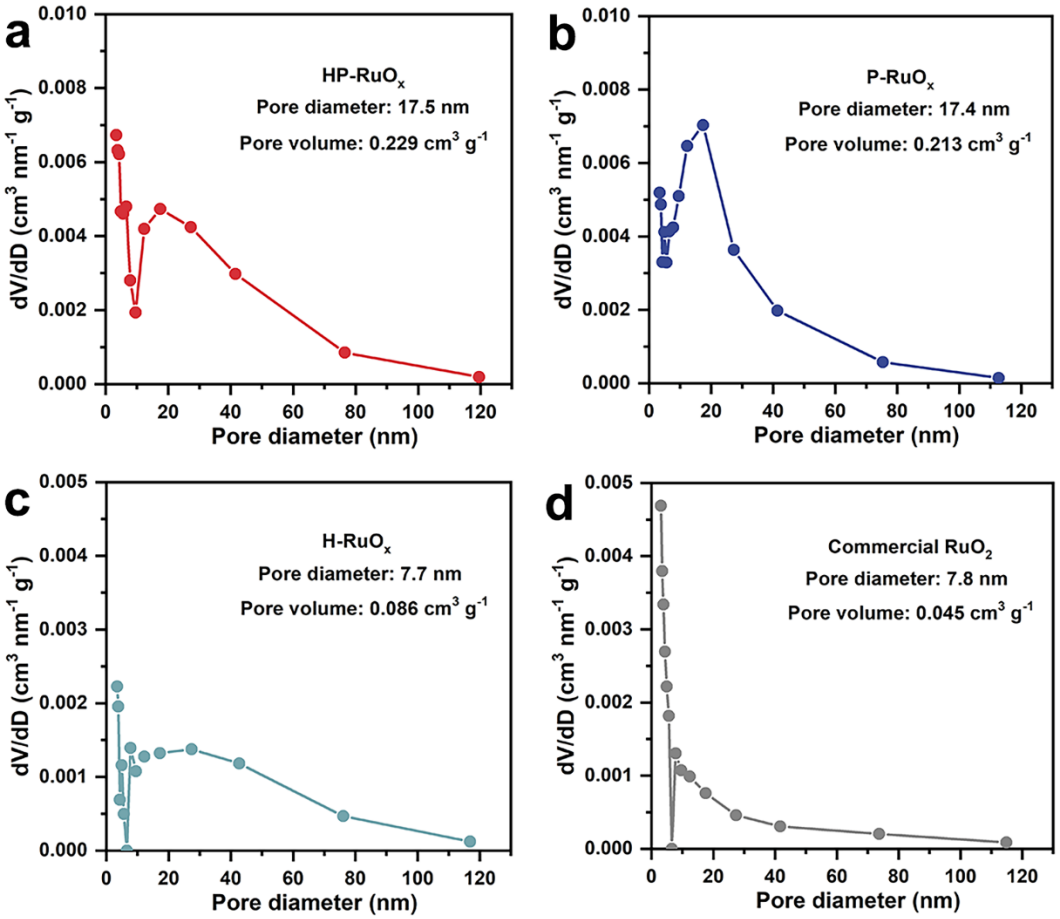

Fig. S12 Pore size and pore volume analyses of (a) HP-RuO_x, (b) P-RuO_x, (c) H-RuO_x, and (d) commercial RuO_2, based on the N_2 desorption isotherms using the BJH method.

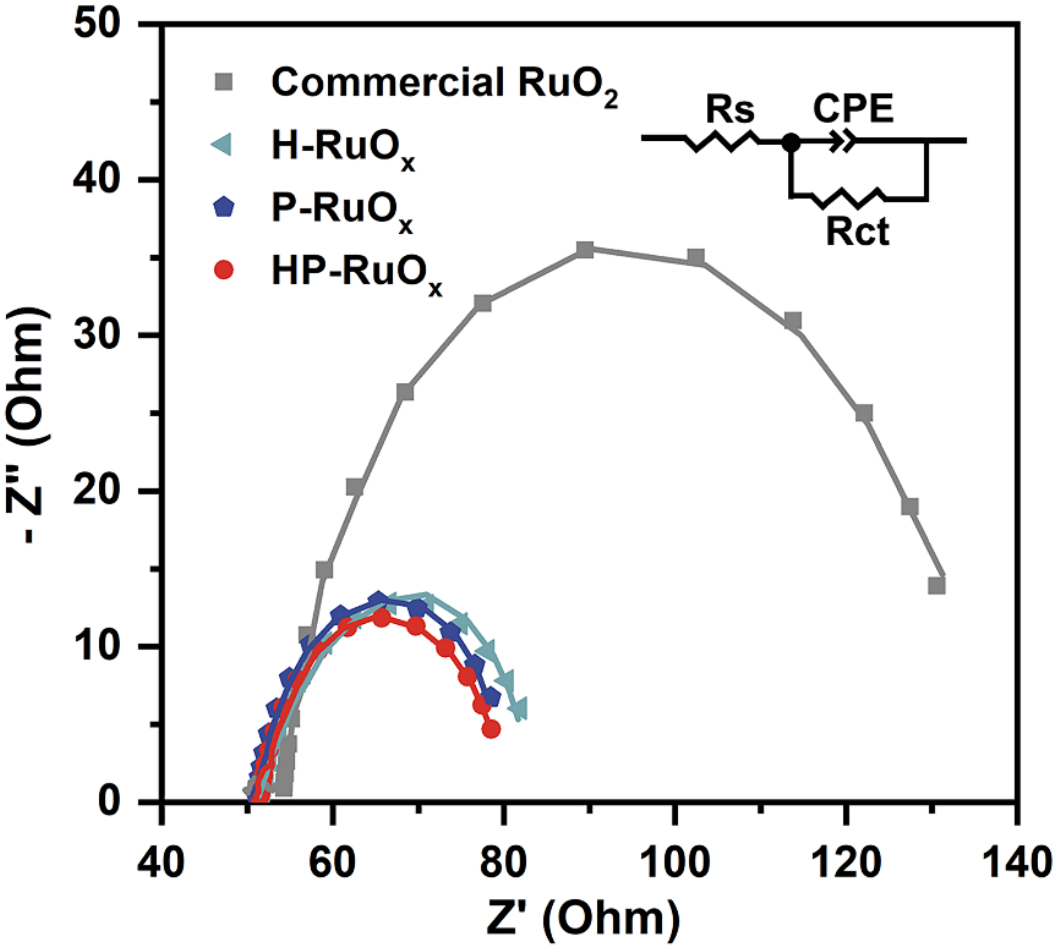

Fig. S13 EIS Nyquist plots of HP-RuO_x, P-RuO_x, H-RuO_x, and commercial RuO_2. The inset shows an equivalent circuit model, in which CPE, R_{ct}, and R_s are constant phase element, charge transfer resistance and equivalent series resistance, respectively. The quantitative fitting results are presented in **Table S1**.

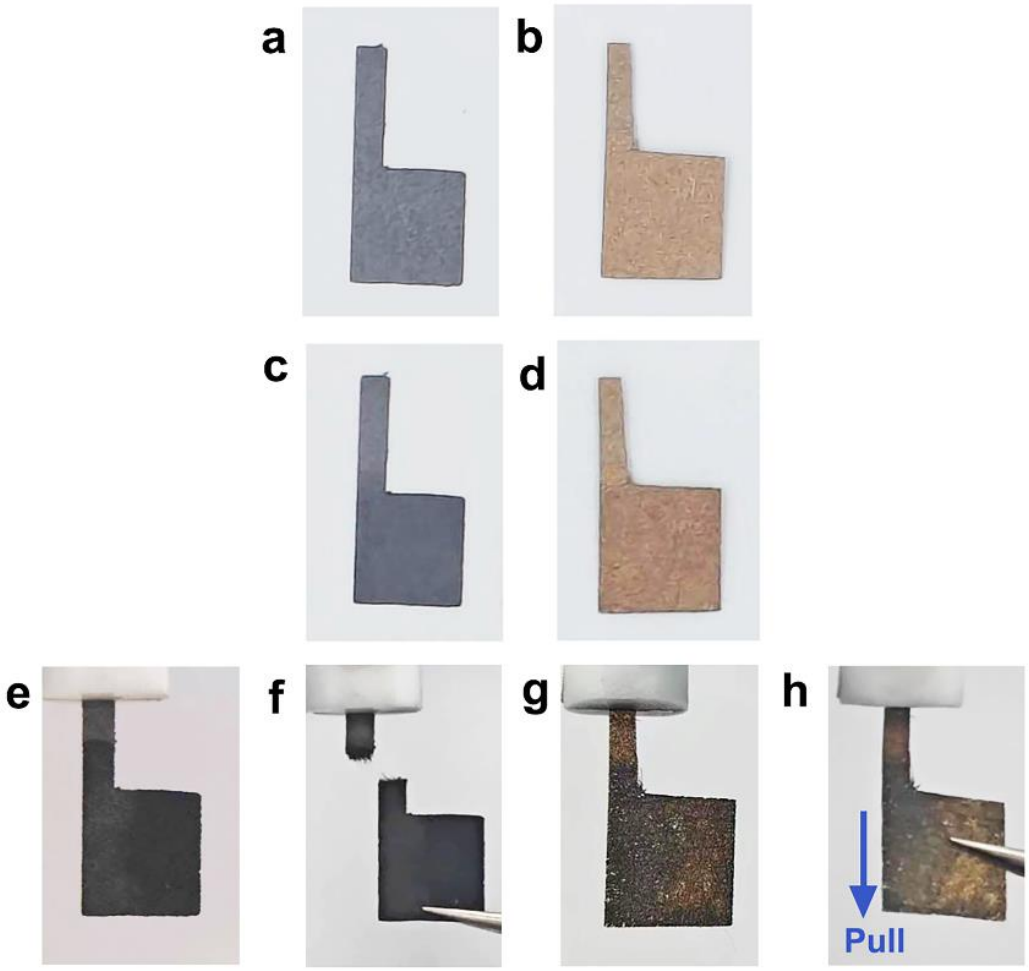

Fig. S14 Digital photographs of (a) a blank carbon paper, (b) a blank Ti@Au felt, (c) a commercial RuO_2 catalyst-loaded carbon paper, and (d) a commercial RuO_2 catalyst-loaded Ti@Au felt. (e, f) The commercial RuO_2 catalyst-loaded carbon paper after a long-term OER test at 100 mA cm^{-2} for 4 h. The carbon paper was oxidized and became rather fragile. (The carbon paper was broken upon a very gentle touch by tweezers) (g, h) The commercial RuO_2 catalyst-loaded Ti@Au felt after a long-term OER test at 100 mA cm^{-2} for 4 h. Although the Au on the surface was partially oxidized and dissolved, the electrode still maintained mechanically robust and showed good electrical conductivity.

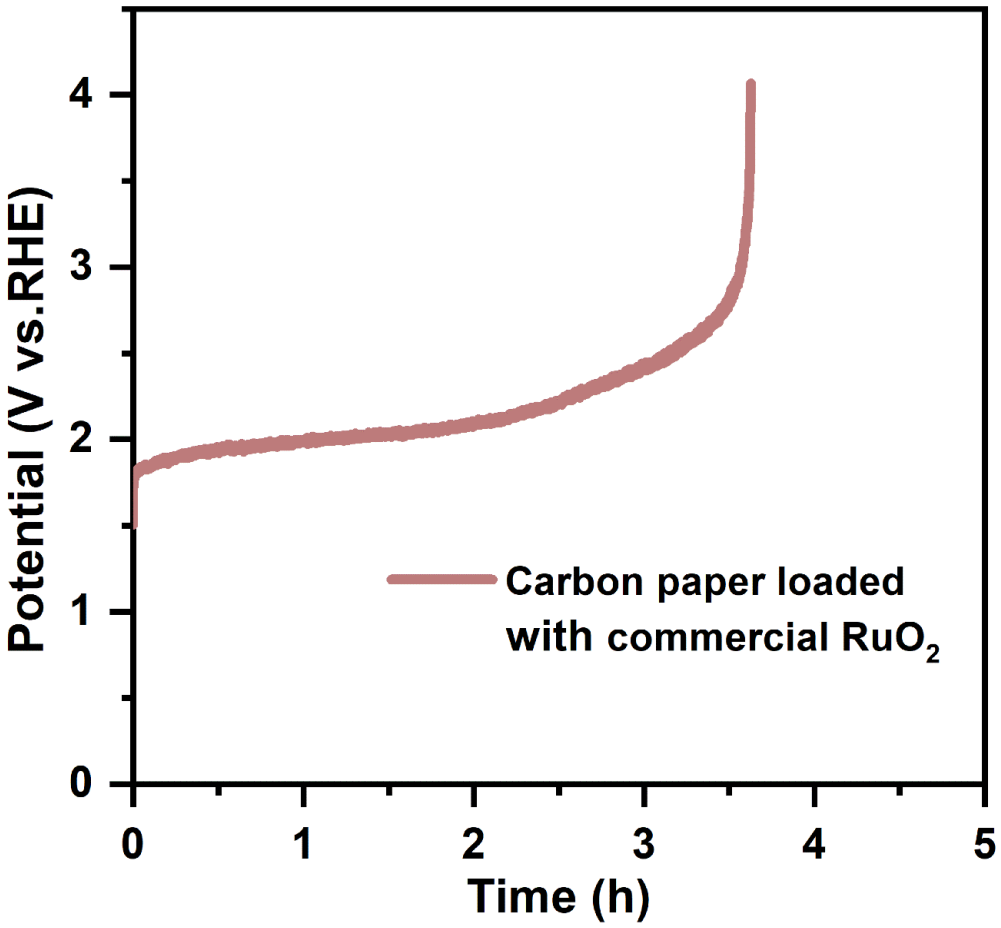

Fig. S15 Chronopotentiometry curve of commercial RuO_2 catalysts loaded on a carbon paper current collector for OER in 0.05 M H_2SO_4 at 100 mA cm^{-2} (loading: 1.0 mg_{cat} cm^{-2}).

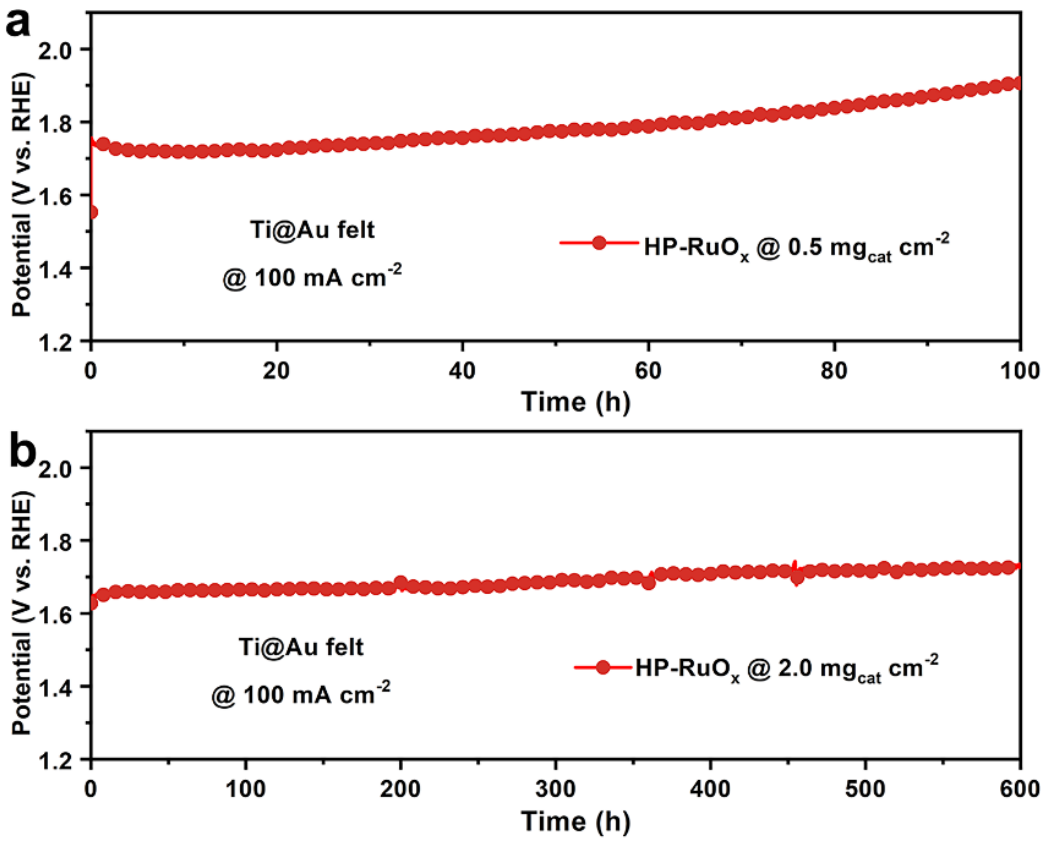

Fig. S16 Chronopotentiometry curves of the HP-RuO_x catalysts for the OER tested in 0.05 M H_2SO_4 at 100 mA cm^{-2} with the catalyst loading of (a) 0.5 mg_{cat} cm^{-2} and (b) 2.0 mg_{cat} cm^{-2}.

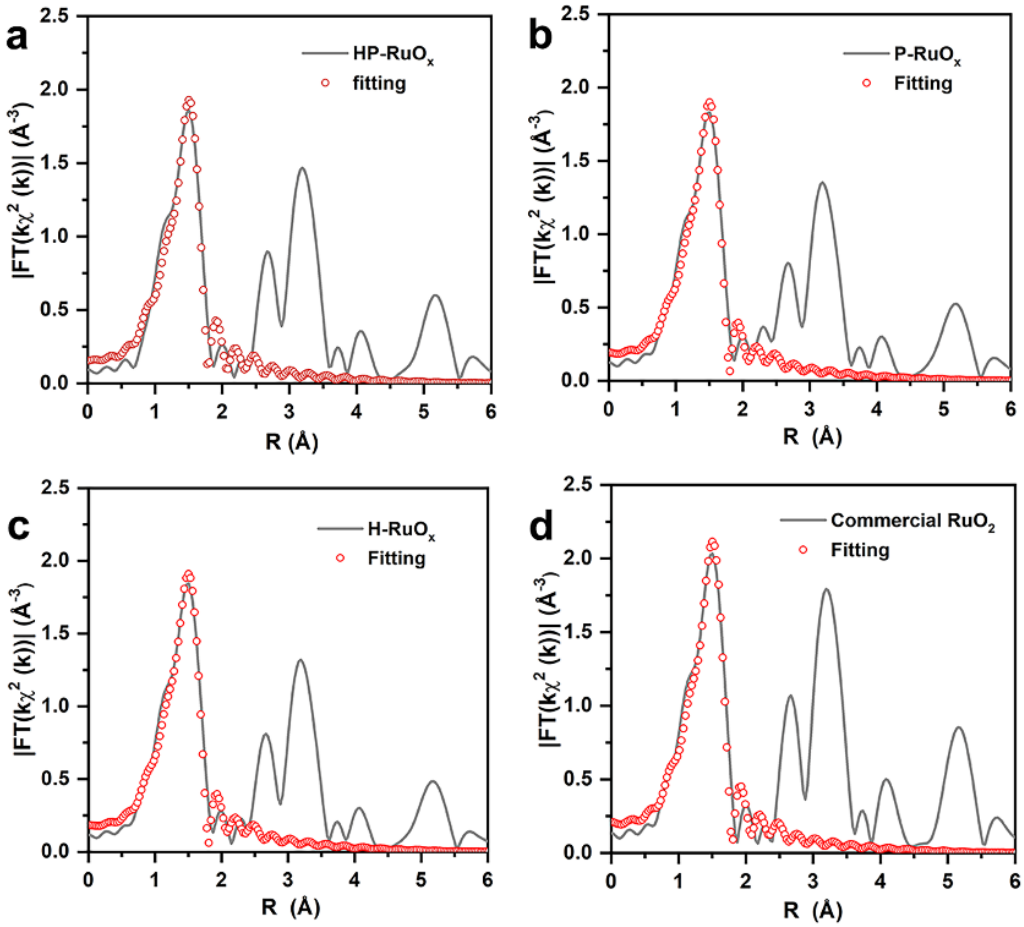

Fig. S17 EXAFS fitting of the first-shell coordination for (a) HP-RuO_x, (b) P-RuO_x, (C) H-RuO_x, and (d) commercial RuO_2 catalysts. The quantification results are shown in **Table S3**.

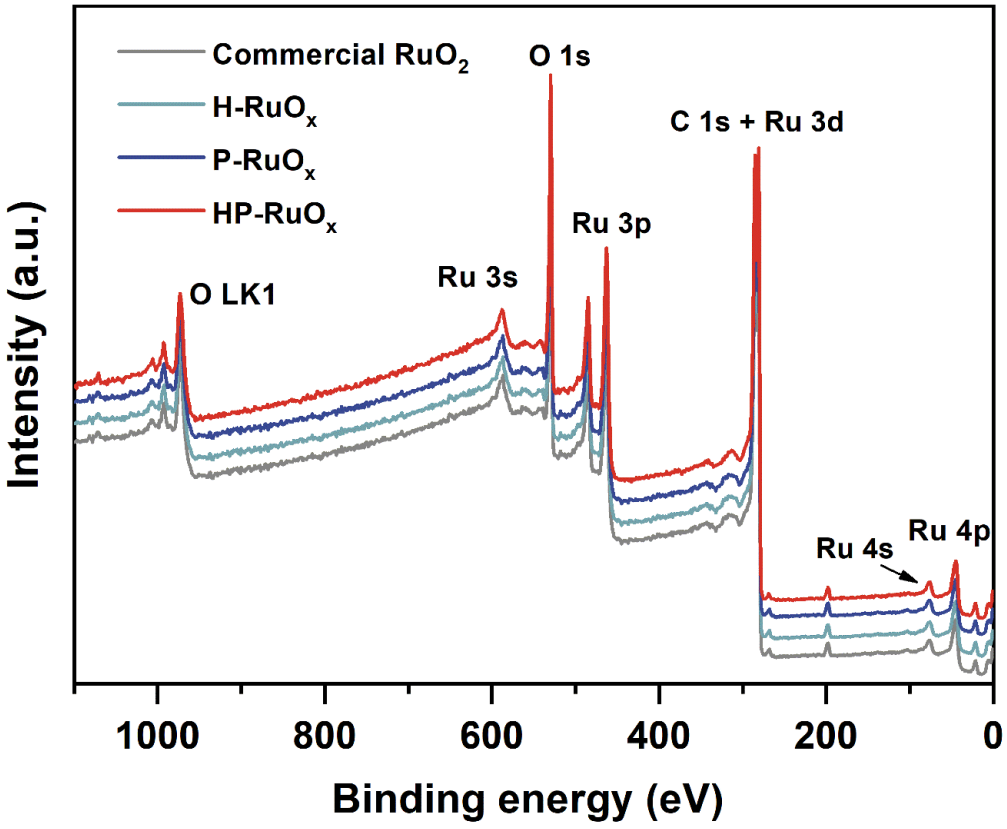

Fig. S18 XPS survey spectra of HP-RuO_x, P-RuO_x, H-RuO_x and commercial RuO_2.

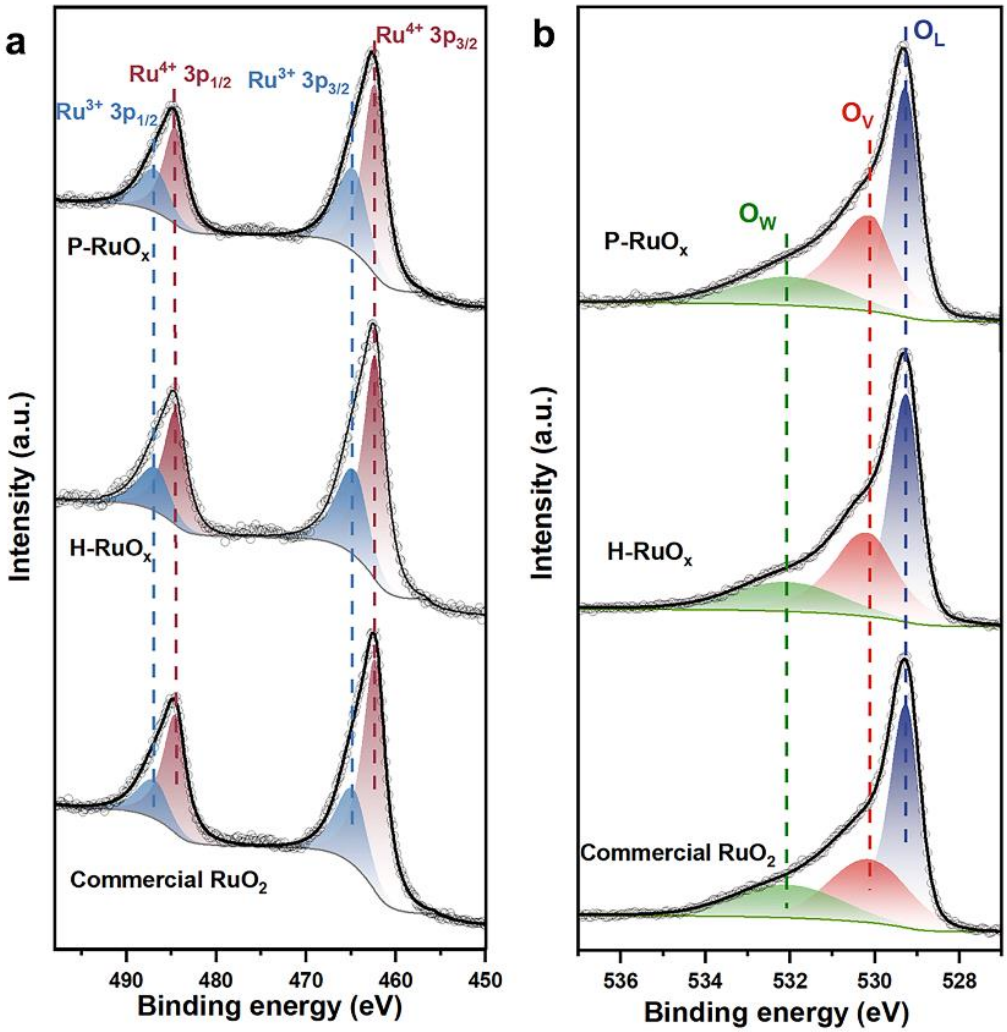

Fig. S19 (a) High-resolution Ru 3p spectra of P-RuO_x, H-RuO_x, and commercial RuO_2. (b) High-resolution O 1s spectra of P-RuO_x, H-RuO_x, and commercial RuO_2. O_L – lattice oxygen, O_V – oxygen vacancy, and O_W – adsorbed oxygen from water.

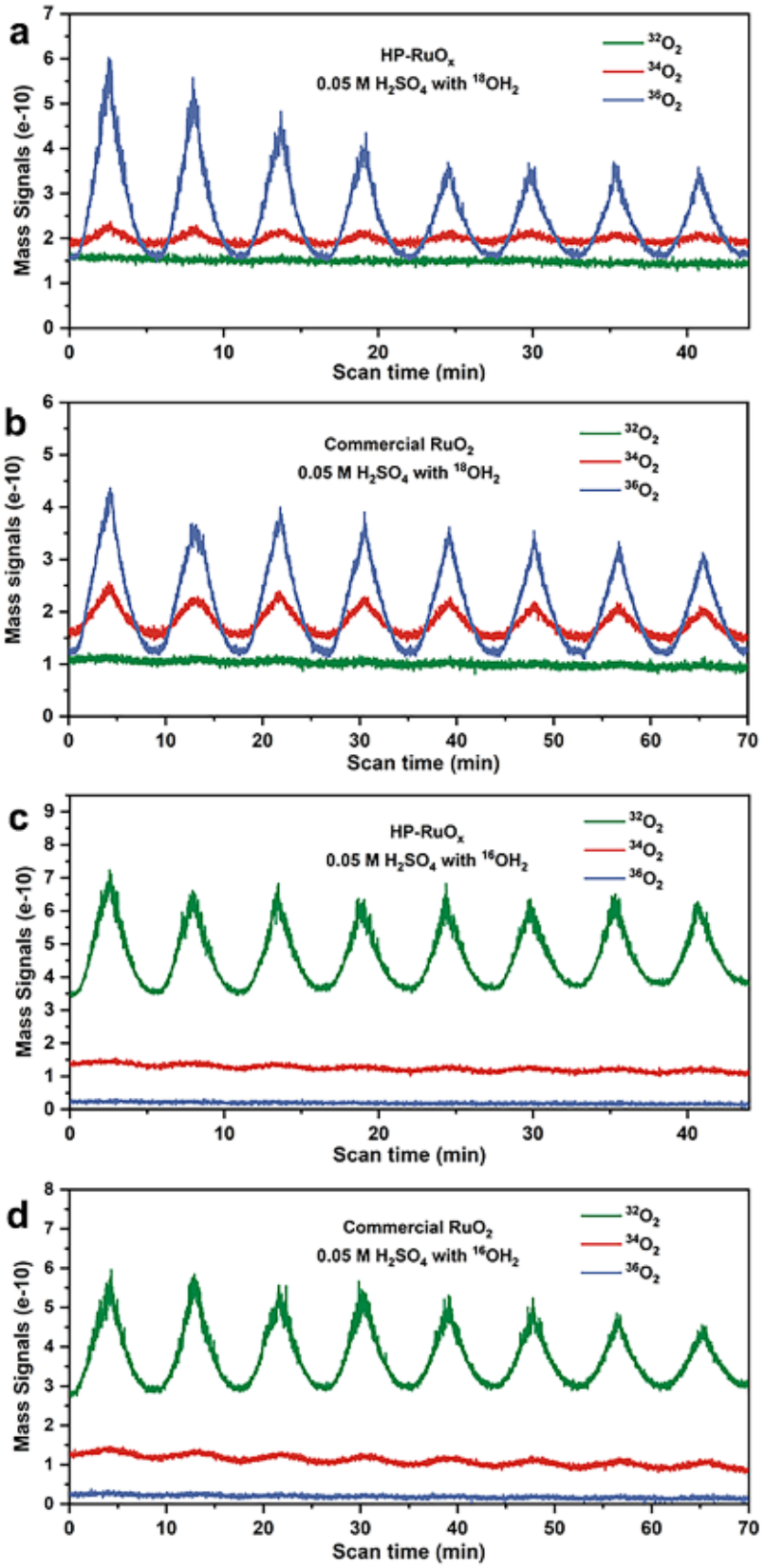

Fig. S20 DEMS measurements of (a) HP-RuO_x and (b) commercial RuO_2 in 0.05 M H_2SO_4 containing $^{18}OH_2$. DEMS measurements of ^{18}O-labeled (c) HP-RuO_x and (d) commercial RuO_2 in 0.05 M H_2SO_4 prepared with $^{16}OH_2$.

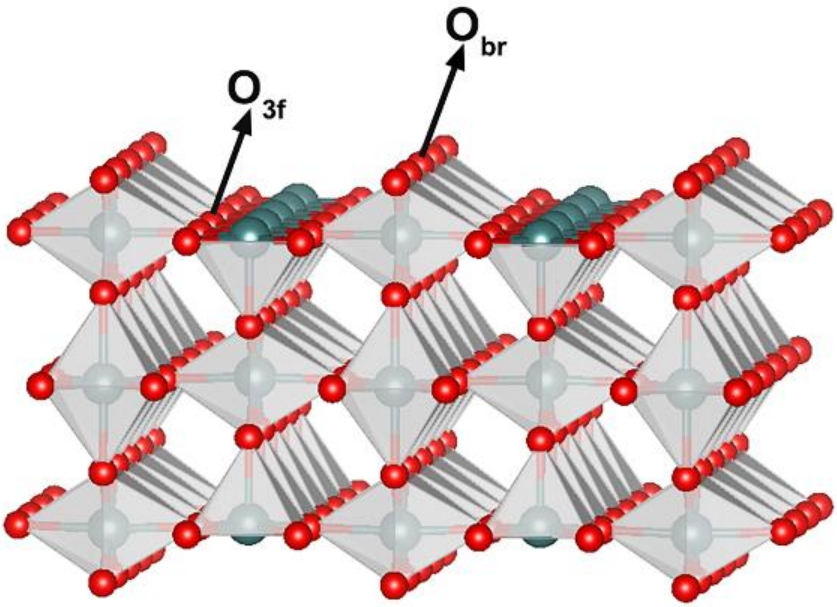

Fig. S21 The model of a perfect $RuO_2(110)$ surface. The red and dark green spheres represent O and Ru atoms, respectively. The outermost O atoms are bridge atoms, labeled as O_{br}, and other O atoms are threefold, labeled as O_{3f}.

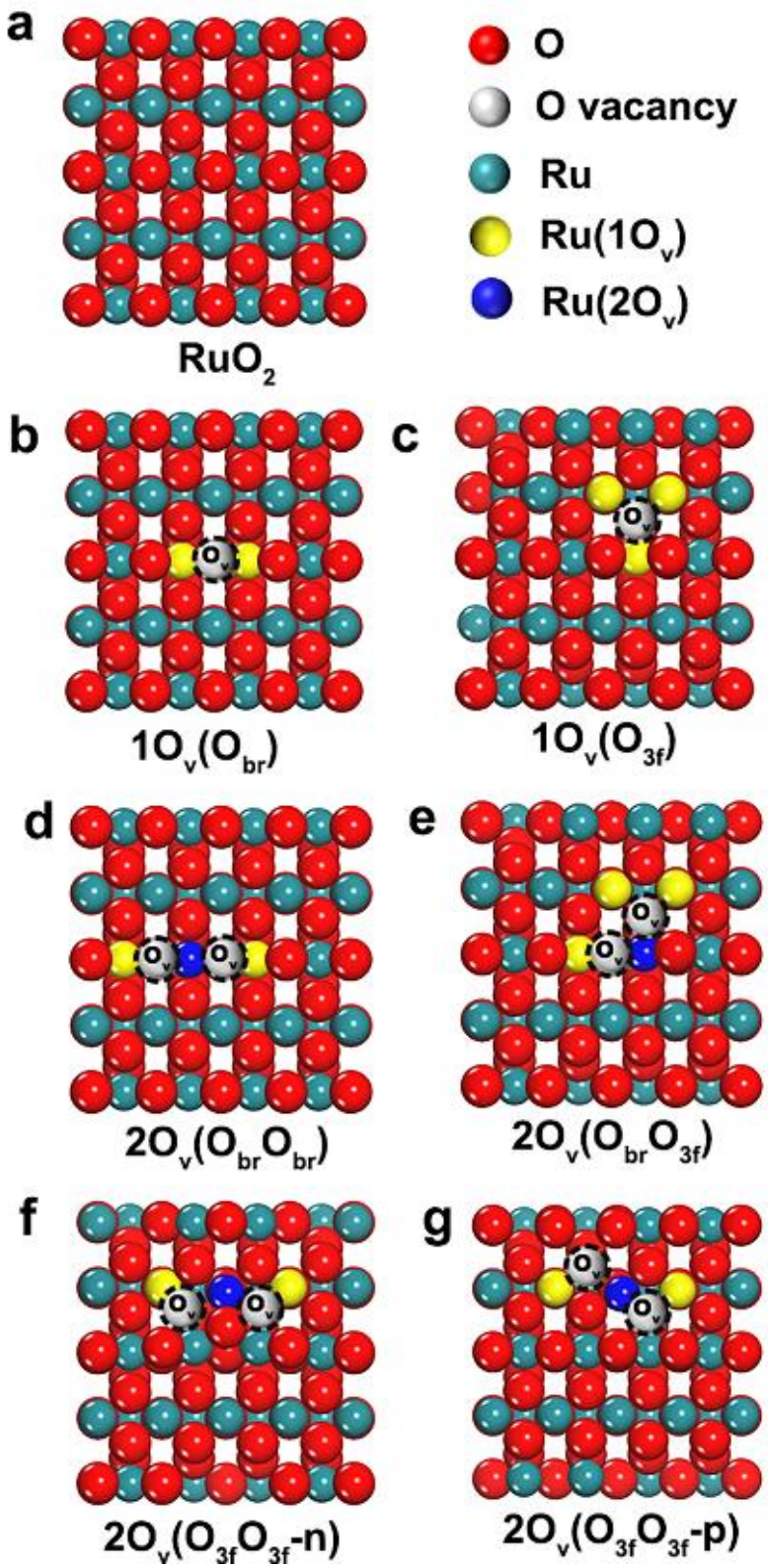

Fig. S22 Top views of (a) the defect-free RuO_2 model, (b - c) two $1O_v$-RuO_x models, and (d - g) four possible $2O_v$-RuO_x models. n and p stand for different relative positions between Ru atom and oxygen vacancies.

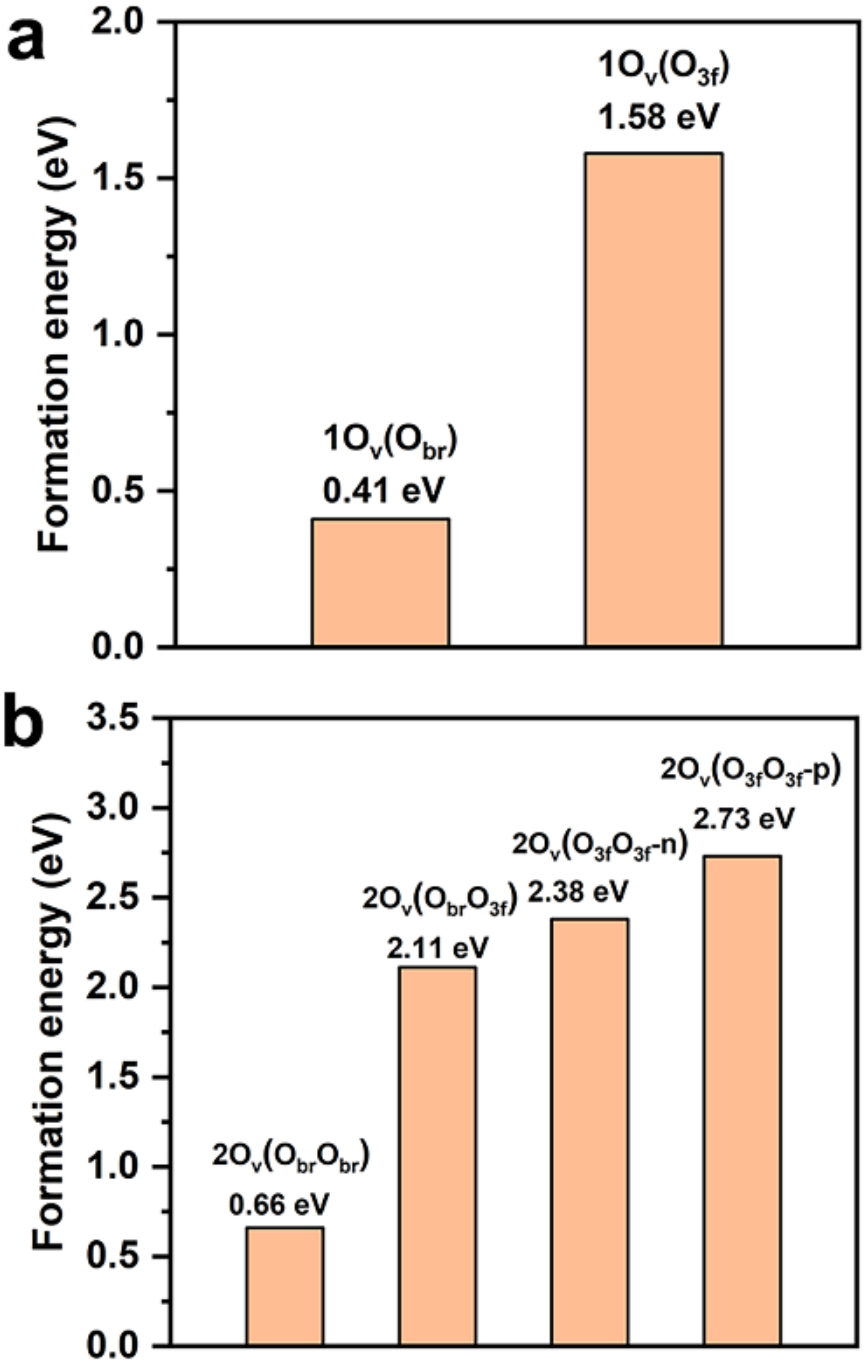

Fig. S23 The formation energy values for the (a) $1O_v$-RuO_x and (b) $2O_v$-RuO_x model catalysts shown in **Fig. S22**.

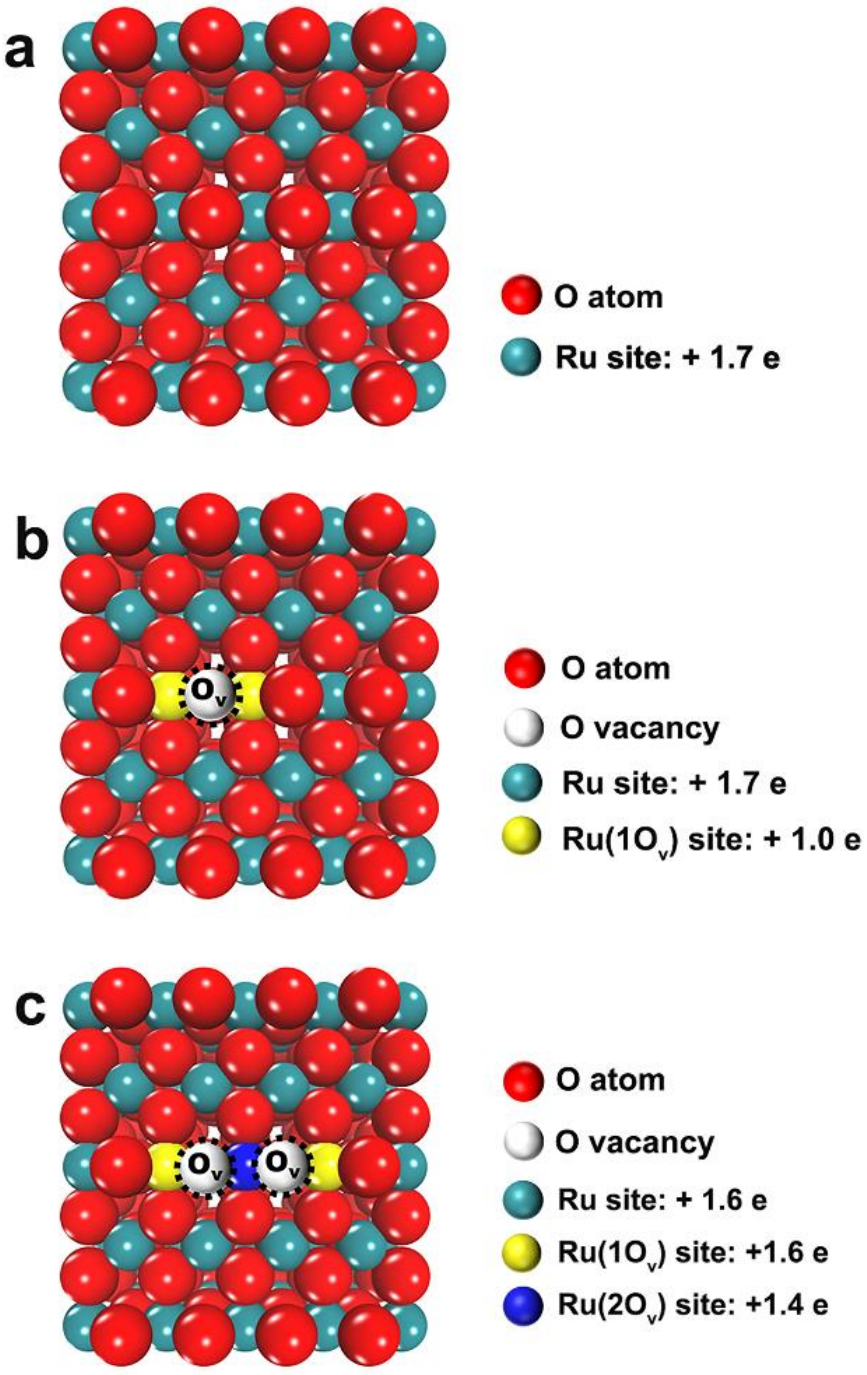

Fig. S24 Bader charge analysis of the Ru sites on (a) pristine RuO_2, (b) $1O_v$-RuO_x and (c) $2O_v$-RuO_x. The dark green, yellow and blue spheres represent unsaturated Ru sites on the RuO_2 (110) surface, Ru sites around a single oxygen vacancy (Ru($1O_v$)) and Ru sites surrounded by dual oxygen vacancies (Ru($2O_v$)). The red and white spheres denote O atoms and oxygen vacancies (O_v), respectively.

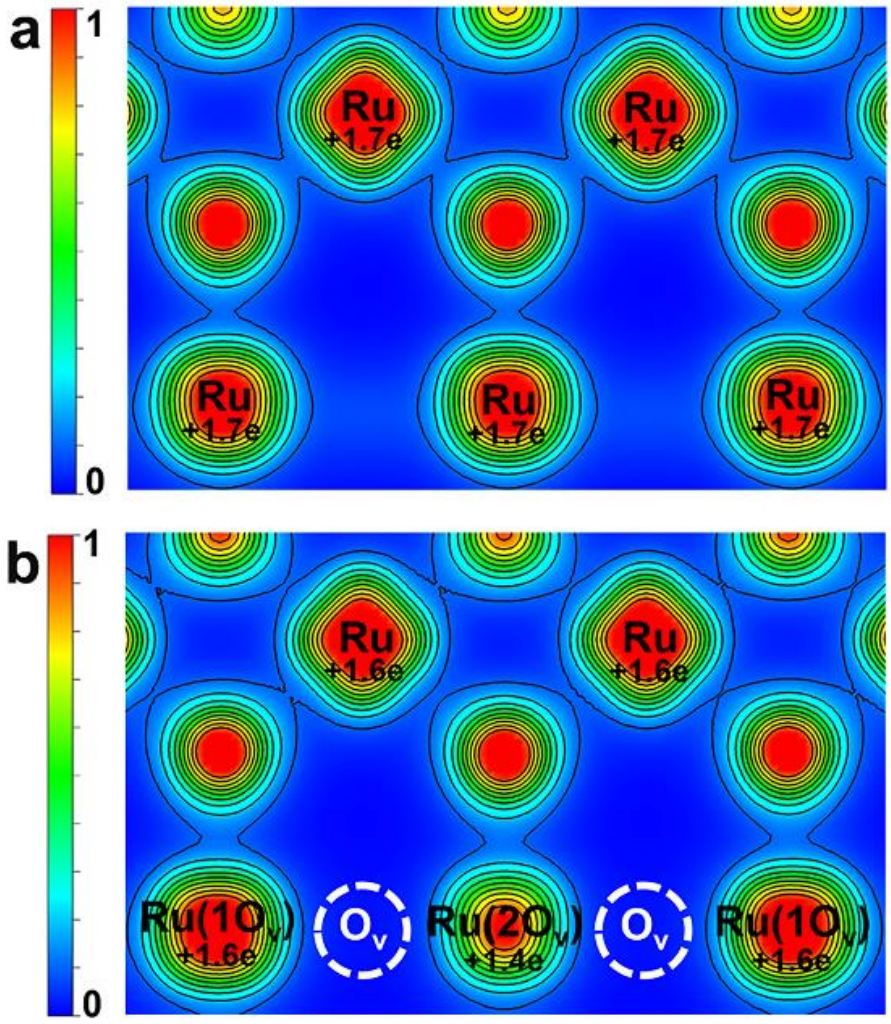

Fig. S25 Two-dimensional charge density contour plots for Ru and O in (a) defect-free RuO_2 and (b) $2O_v$-RuO_x.

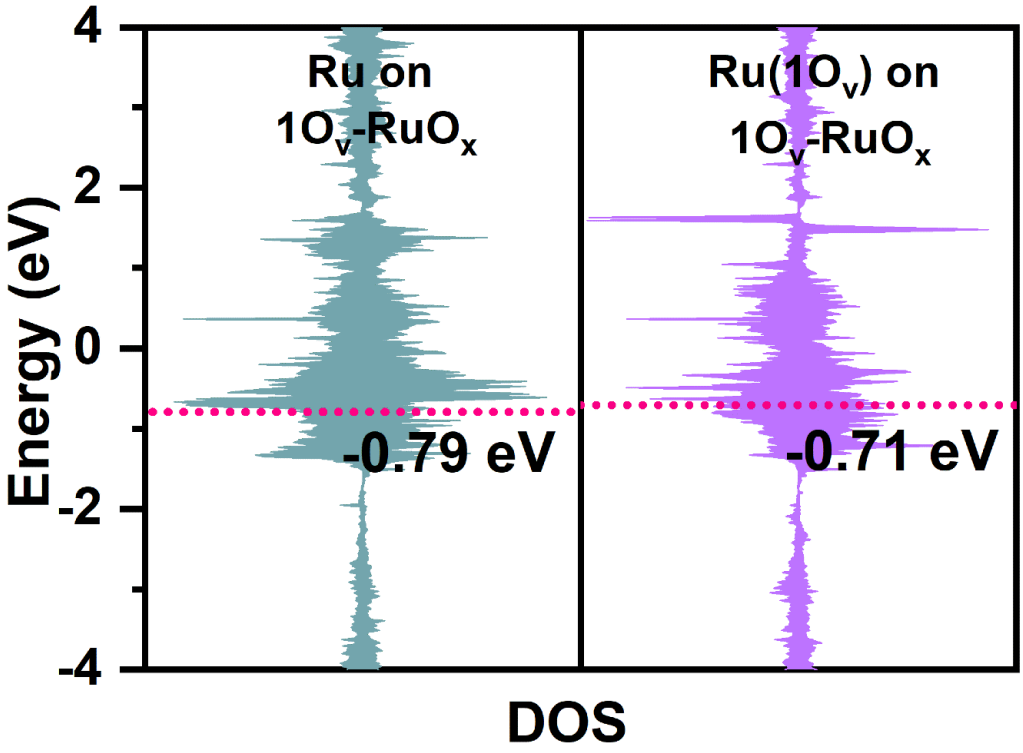

Fig. S26 Partial density of states (PDOS) analysis of the Ru sites on $1O_v$-RuO_x. Ru and Ru($1O_v$) represent the unsaturated Ru sites on the RuO_2 (110) surface and Ru sites around a single oxygen vacancy, respectively.

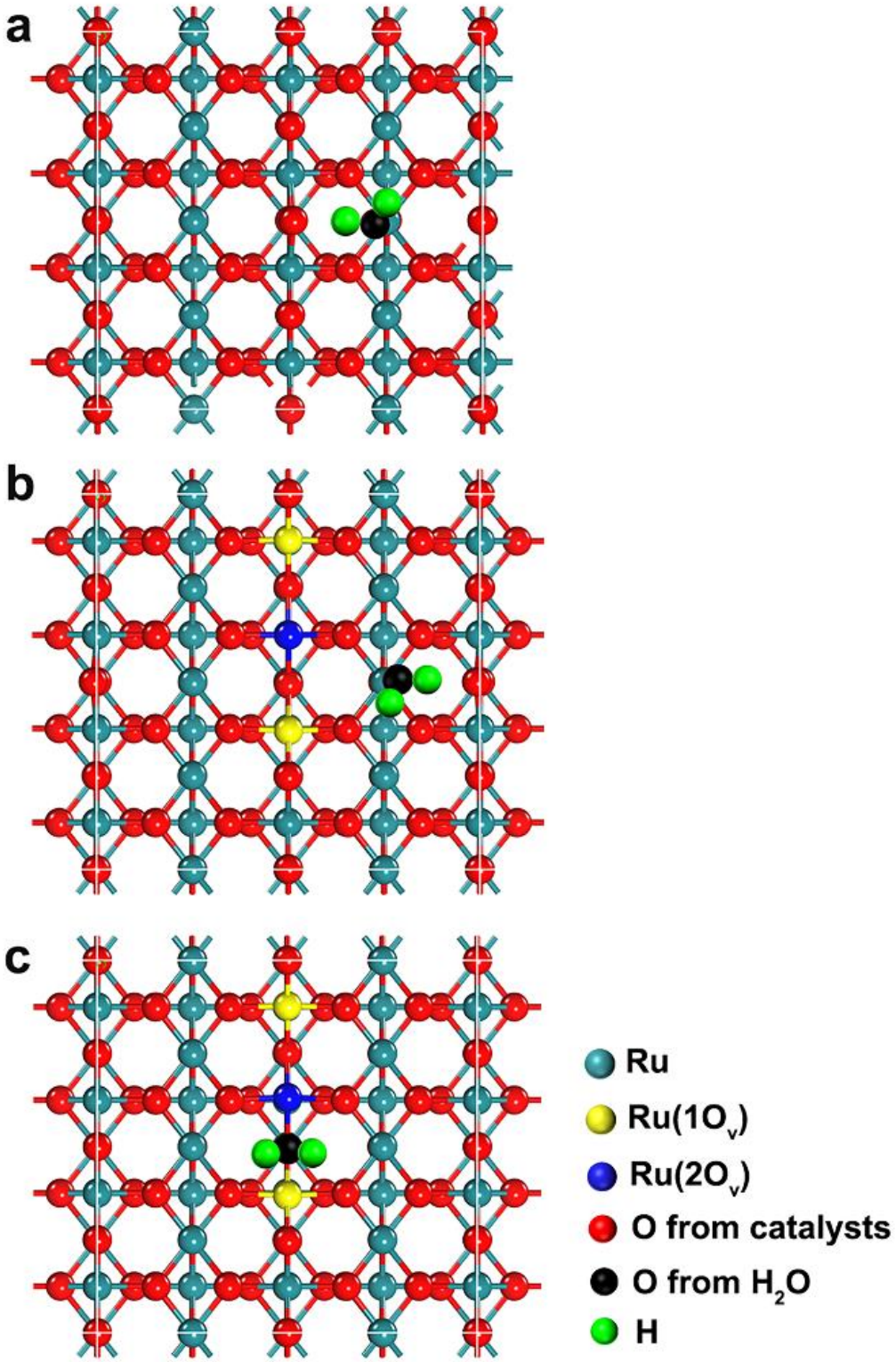

Fig. S27 Top view images showing H_2O adsorption on the (a) Ru site of RuO_2, (b) Ru($2O_v$) site of $2O_v$-RuO_x, and (c) O_v site of $2O_v$-RuO_x.

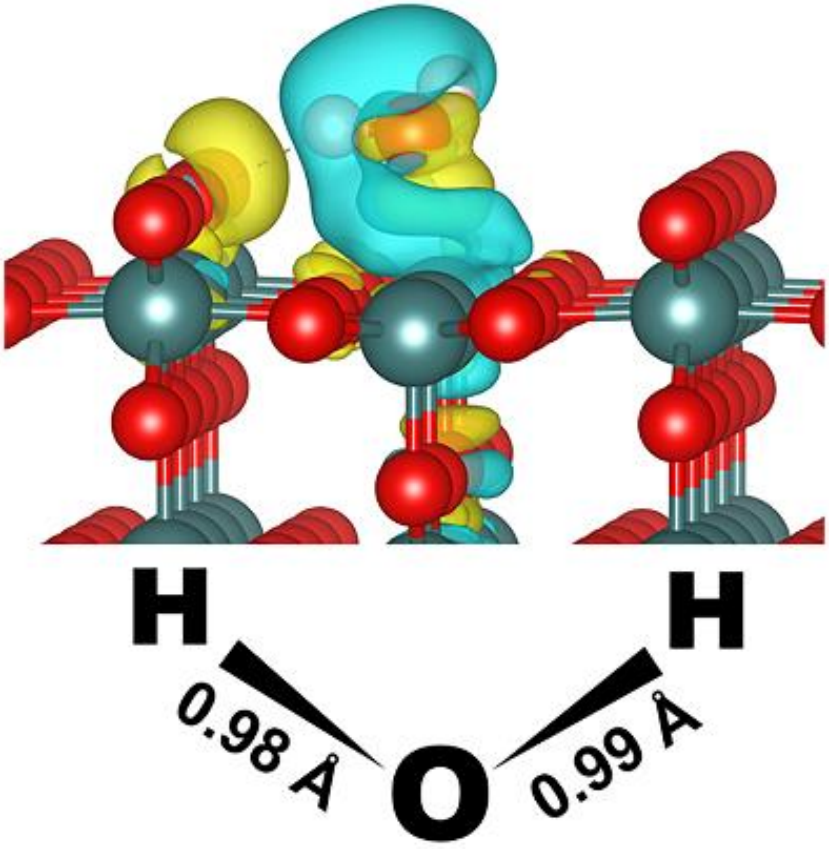

Fig. S28 The charge density difference plot for H_2O adsorption on the Ru sites of RuO_2. The yellow and cyan regions represent electron accumulation and depletion, respectively. The isosurface value is 0.001 e/Bohr^3.

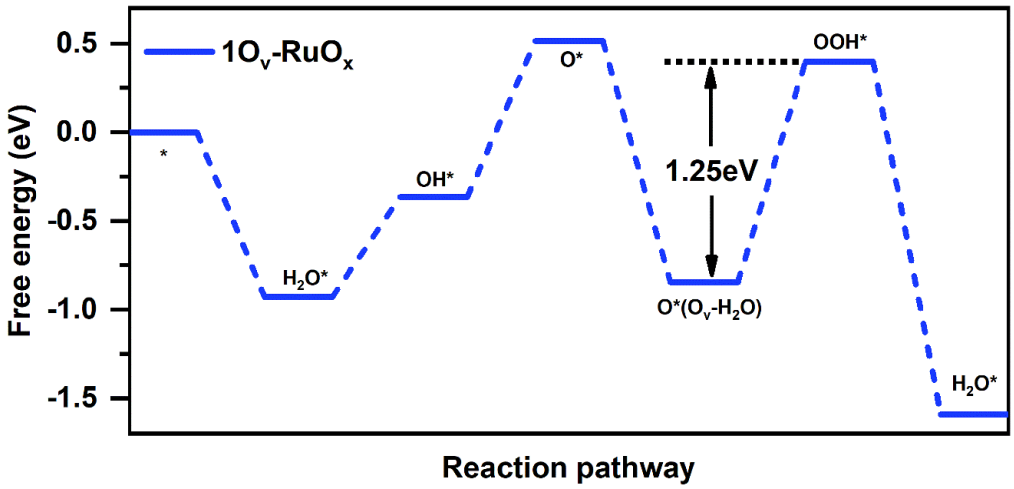

Fig. S29 The Gibbs free-energy diagram for the OER on $1O_v$-RuO_x.

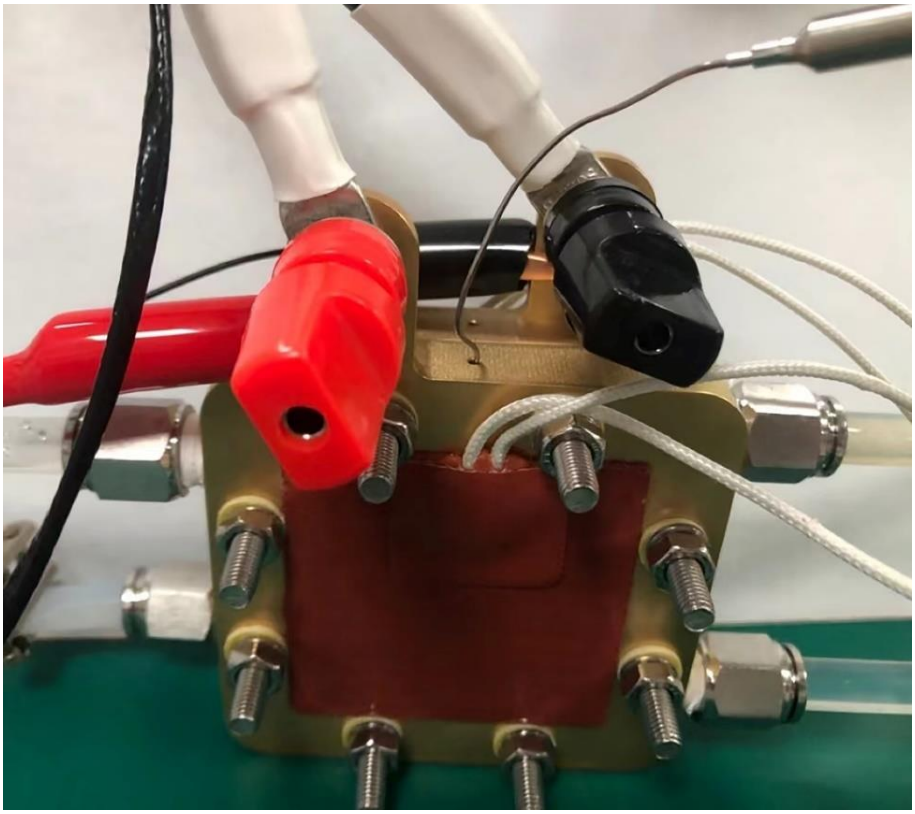

Fig. S30 Digital photograph showing the PEM single-cell electrolyzer used in our experiments.

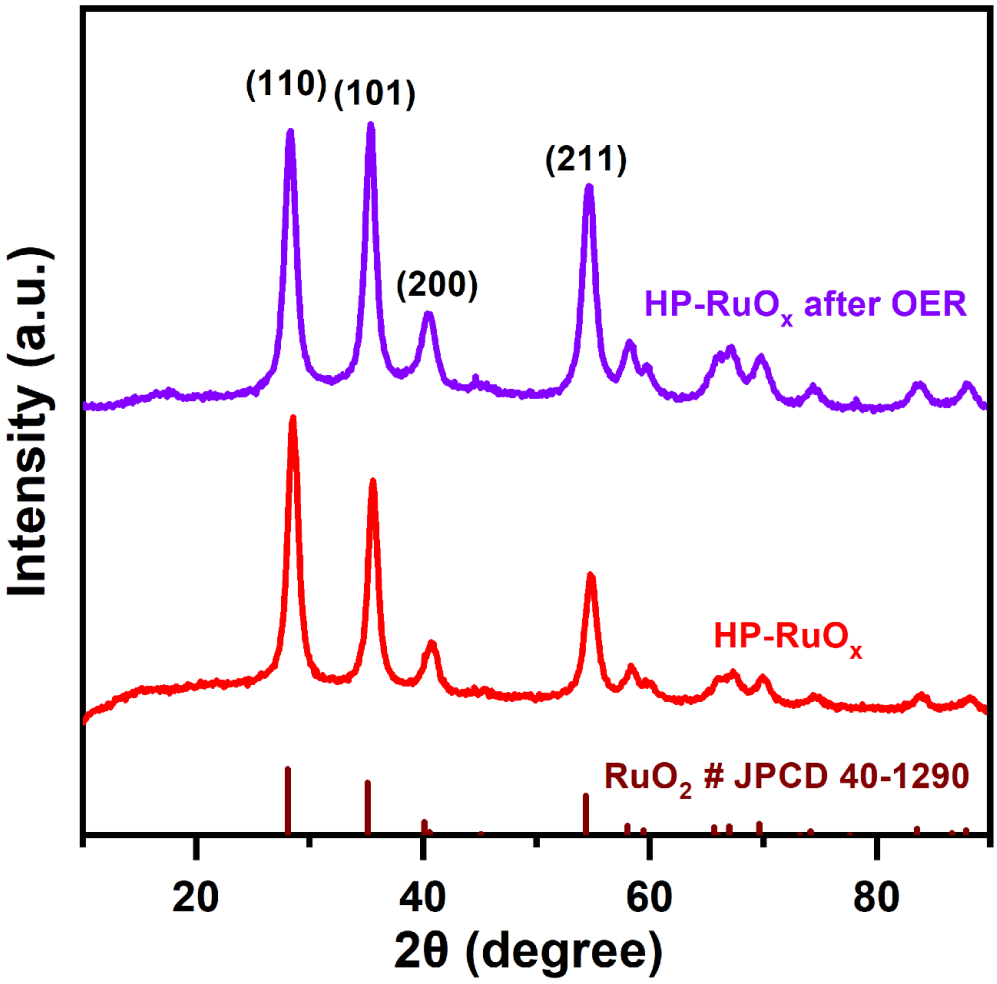

Fig. S31 XRD patterns of HP-RuO_x catalysts before and after the OER at 500 mA cm^{-2} for 150 h in MEA.

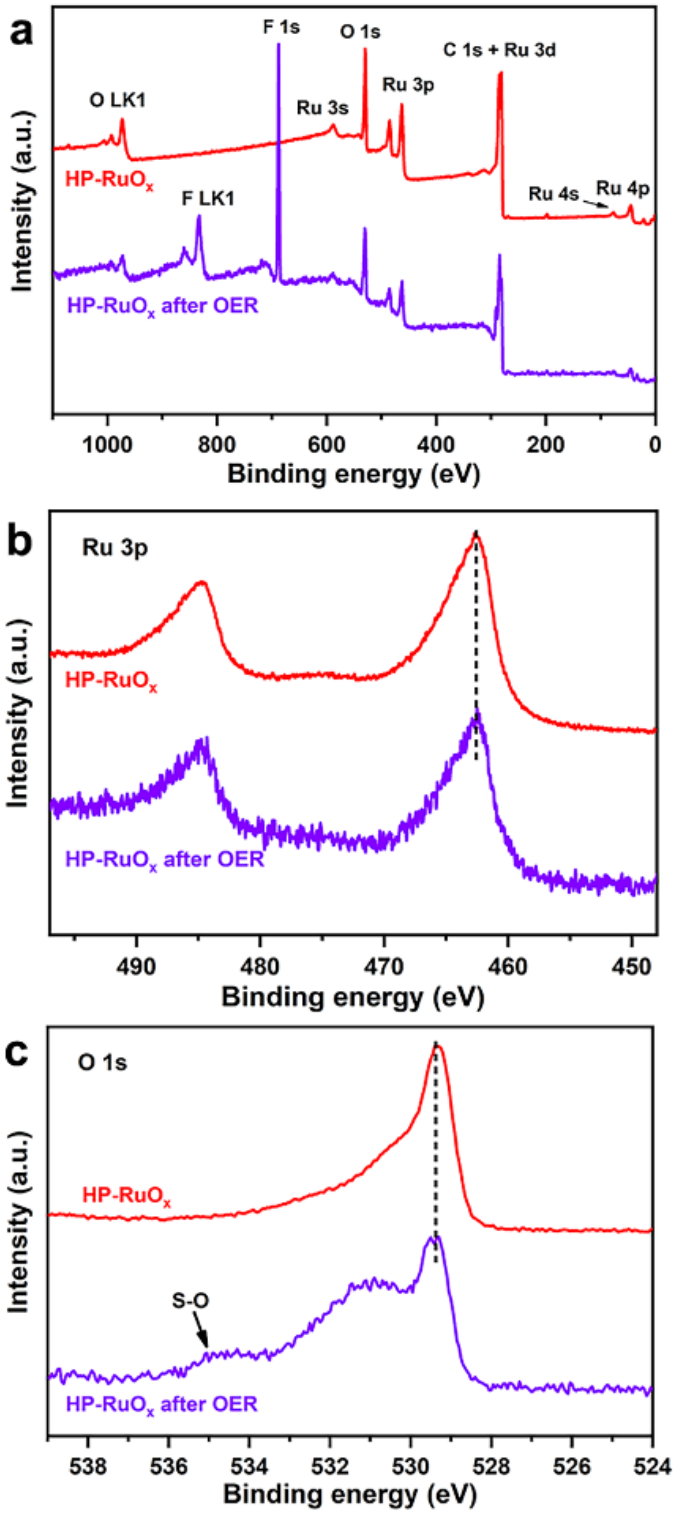

Fig. S32 (a) XPS survey spectra, high-resolution (b) Ru 3p and (c) O 1s XPS spectra of HP-RuO_x catalysts before and after the OER at 500 mA cm^{-2} for 150 h in MEA. The F signal in (a) comes from the remanent Nafion used to prepare the catalyst ink. Since Nafion ($C_7HF_{13}O_5SC_2F_4$) is very difficult to be removed completely, it may also influence the (quantitative) analysis of the O 1s spectrum after the stability test.

Supplementary Tables:

Table S1. EIS Fitting results of R_s and R_{ct} values for different samples.

Sample	R_s (Ω)	R_{ct} (Ω)
Commercial RuO_2	54.1	80.1
H-RuO_x	51.8	32.9
P-RuO_x	51.3	30.0
HP-RuO_x	51.3	29.2

R_s – equivalent series resistance.

R_{ct} – charge transfer resistance.

Table S2. Summary of some Ru-based OER electrocatalysts reported recently in the literature, which were tested in acidic electrolyte.

Catalysts	Electrolyte	Activity (η_{10}, mV)	Stability	Reference
HP-RuO_x	**0.05 M H_2SO_4**	**237**	**140 h @ 100 mA cm^{-2}**	**This work**
RuO_2 NSs	0.1 M $HClO_4$	255	6 h @ 10 mA cm^{-2}	Ref. S1
a/c-RuO_2	0.1 M $HClO_4$	220	60 h @ 10 mA cm^{-2}	Ref. S2
Ru_1-Pt_3Cu	0.1 M $HClO_4$	220	28 h @ 10 mA cm^{-2}	Ref. S3
Co-RuIr	0.1 M $HClO_4$	235	25 h @ 10 mA cm^{-2}	Ref. S4
RuB_2	0.5 M H_2SO_4	223	45 h @ 10 mA cm^{-2}	Ref. S5
RuIr@CoNC	0.05 M H_2SO_4	239	25 h @ 10 mA cm^{-2}	Ref. S6
Ru@IrO_x	0.05 M H_2SO_4	282	24 h @ 10 mA cm^{-2}	Ref. S7
Ru-exchanged Cu-BTC	0.5 M H_2SO_4	188	8 h @ 10 mA cm^{-2}	Ref. S8
$Y_{1.7}Sr_{0.3}Ru_2O_7$	0.5 M H_2SO_4	264	28 h @ 10 mA cm^{-2}	Ref. S9
Ru/RuS_2	0.5 M H_2SO_4	201	24 h @ 10 mA cm^{-2}	Ref. S10
Ru@$MoO(S)_3$	0.5 M H_2SO_4	292	24 h @ 10 mA cm^{-2}	Ref. S11
RuO_2-WC NPs	0.5 M H_2SO_4	347	10 h @ 10 mA cm^{-2}	Ref. S12
La-RuO_2	0.5 M H_2SO_4	208	28 h @ 10 mA cm^{-2}	Ref. S13
$RuCoO_x$@LLCF	0.1 M $HClO_4$	256	110 h @ 10 mA cm^{-2}	Ref. S14
Y_2MnRuO_7	0.1 M $HClO_4$	270	45 h @ 10 mA cm^{-2}	Ref. S15
Ru/Se-RuO_2	0.5 M H_2SO_4	190	24 h @ 10 mA cm^{-2}	Ref. S16
$Ru_{0.85}Zn0.15O_{2-\delta}$	0.5 M H_2SO_4	190	50 h @ 10 mA cm^{-2}	Ref. S17
$RuTe_2$ PNRs	0.5 M H_2SO_4	245	24 h @ 10 mA cm^{-2}	Ref. S18
C-RuO_2-RuSe-5	0.5 M H_2SO_4	212	50 h @ 10 mA cm^{-2}	Ref. S19
SnRuO_x	0.5 M H_2SO_4	194	250 h @ 100 mA cm^{-2}	Ref. S20
L-Ru	0.5 M H_2SO_4	202	10 h @ 10 mA cm^{-2}	Ref. S21
$RuNi_2$©G-250	0.5 M H_2SO_4	227	24 h @ 10 mA cm^{-2}	Ref. S22
Mg-RuO2	0.5 M H_2SO_4	228	30 h @ 10 mA cm^{-2}	Ref. S23
$Co_{0.11}Ru_{0.89}O_{2-\delta}$	0.5 M H_2SO_4	169	50 h @ 10 mA cm^{-2}	Ref. S24

$RuCoO_x$-RuCo-NC	0.5 M H_2SO_4	228	12 h @ 10 mA cm^{-2}	Ref. S25
$IrRu/T_{90}G_{10}$	0.1 M $HClO_4$	254	24 h @ 10 mA cm^{-2}	Ref. S26
RuMn	0.5 M H_2SO_4	270	720 h @ 10 mA cm^{-2}	Ref. S27
Ru/Co-N-C	0.5 M H_2SO_4	232	24 h @ 10 mA cm^{-2}	Ref. S28
Ru/MnO_2	0.1 M $HClO_4$	161	200 h @ 10 mA cm^{-2}	Ref. S29
$Mn_{0.73}Ru_{0.27}O_{2-\delta}$	0.5 M H_2SO_4	208	10 h @ 10 mA cm^{-2}	Ref. S30
$In_{0.17}Ru_{0.83}O_2$-350	0.5 M H_2SO_4	177	20 h @ 10 mA cm^{-2}	Ref. S31
$Ru_5W_1O_x$	0.5 M H_2SO_4	227	550 h @ 10 mA cm^{-2}	Ref. S32
Co_{CV}/np-RuO_2-250	0.5 M H_2SO_4	169	20 h @ 10 mA cm^{-2}	Ref. S33
Ru/RuO_2-Co_3O_4	0.1 M $HClO_4$	226	20 h @ 10 mA cm^{-2}	Ref. S34
H/d-MnO_x/RuO_2	0.5 M H_2SO_4	178	40 h @ 10 mA cm^{-2}	Ref. S35
$Nd_{0.1}RuO_x$	0.5 M H_2SO_4	211	25 h @ 10 mA cm^{-2}	Ref. S36
Ru-VO_2	0.5 M H_2SO_4	300	125 h @ 10 mA cm^{-2}	Ref. S37
(Ru-W)O_x	0.5 M H_2SO_4	170	300 h @ 10 mA cm^{-2}	Ref. S38
Ru-O-Mn/CPD	0.5 M H_2SO_4	196	30 h @ 10 mA cm^{-2}	Ref. S39
RuO_2/CeO_2@C	0.5 M H_2SO_4	170	100 h @ 50 mA cm^{-2}	Ref. S40
Ru-UiO-67-bpydc	0.5 M H_2SO_4	200	140 h @ 50 mA cm^{-2}	Ref. S41
$Bi_{0.15}Ru_{0.85}O_2$	0.5 M H_2SO_4	200	100 h @ 10 mA cm^{-2}	Ref. S42
$RuCoO_x$	1.0 M $HClO_4$	200	100 h @ 10 mA cm^{-2}	Ref. S43
$Nb_{0.1}Ru_{0.9}O_2$	0.5 M H_2SO_4	204	360 h @ 200 mA cm^{-2}	Ref. S44
py-RuO_2:Zn	0.5 M H_2SO_4	212	1000 h @ 10 mA cm^{-2}	Ref. S45
$Re_{0.06}Ru_{0.94}O_2$	0.1 M $HClO_4$	190	200 h @ 10 mA cm^{-2}	Ref. S46
$Li_{0.52}$RuO2	0.5 M H_2SO_4	156	70 h @ 10 mA cm^{-2}	Ref. S47
$Bi_xEr_{2-x}Ru_2O_7$	0.1 M $HClO_4$	180	100 h @ 100 mA cm^{-2}	Ref. S48
Ru/TiO_x	0.5 M H_2SO_4	174	900 h @ 10 mA cm^{-2}	Ref. S49
Ni-RuO_2	0.1 M $HClO_4$	214	200 h @ 10 mA cm^{-2}	Ref. S50
Se-RuO_2	0.5 M H_2SO_4	166	48 h @ 10 mA cm^{-2}	Ref. S51
RuFe@CF	0.5 M H_2SO_4	188	620 h @ 10 mA cm^{-2}	Ref. S52
m-RuO_2	0.5 M H_2SO_4	230	4 h @ 10 mA cm^{-2}	Ref. S53
$MnRuO_x$-300	0.5 M H_2SO_4	231	780 h @ 100 mA cm^{-2}	Ref. S54

GB-RuO_2	0.1 M $HClO_4$	187	550 h @ 10 mA cm^{-2}	Ref. S55
$RuSnO_x$	0.1 M $HClO_4$	184	150 h @ 10 mA cm^{-2}	Ref. S56
Ru-RuO_2/Mn_3O_4/CP	0.5 M H_2SO_4	182	400 h @ 10 mA cm^{-2}	Ref. S57
$RuMnO_x$	0.5 M H_2SO_4	240	2600 h @ 10 mA cm^{-2}	Ref. S58
MD-RuO_2-BN	0.5 M H_2SO_4	196	24 h @ 10 mA cm^{-2}	Ref. S59
Si-RuO_2-0.1	0.1 M $HClO_4$	226	800 h @ 10 mA cm^{-2}	Ref. S60

Table S3. Ligand structure parameters derived from EXAFS spectrum fitting.

Sample	CN	R (Å)	σ^2 (Å^2)	ΔE_0	R_{factor}
Commercial RuO_2	6.0	1.97	0.002	-2.99	0.012
H-RuO_x	5.92	1.97	0.002	-3.12	0.010
P-RuO_x	5.51	1.97	0.002	-3.60	0.010
HP-RuO_x	5.26	1.97	0.001	-4.29	0.021

CN − coordination number

R − bond distance

σ^2 − Debye-Waller factors

ΔE_0 − the inner potential correction

R_{factor} − goodness of fit

Table S4. Quantitative XPS analyses of Ru^{3+} species and the oxygen vacancy (O_V).

Sample	Ru^{3+}	O_V
Commercial RuO_2	28.6 %	30.5 %
H-RuO_x	32.9 %	34.6 %
P-RuO_x	38.3 %	39.3 %
HP-RuO_x	42.9 %	41.0 %

Table S5. Gibbs free energy values of H_2O adsorption on defect-free RuO_2, $Ru(2O_v)$ of $2O_v$-RuO_x, and O_v of $2O_v$-RuO_x.

	H (eV)	**ZPE (eV)**	**T × S (T = 298.15 K)**	**G (eV)**	**ΔG （eV）**
RuO_2	-714.06	0.68	0.11	-713.49	-0.96
$Ru(2O_v)$	-703.06	0.68	0.11	-702.49	-0.93
O_v	-702.82	0.67	0.13	-702.28	-0.72

H – enthalpy

ZPE – zero-point energy

T × S – entropy contribution

G − Gibbs free energy

∆G – the change of Gibbs free energy induced by H_2O adsorption

Table S6. Gibbs energy changes of the elementary steps during the OER on RuO_2, $1O_v$-RuO_x and $2O_v$-RuO_x.

U = 0 V	△G (eV) RuO_2	△G (eV) $1O_v$-RuO_x	△G (eV) $2O_v$-RuO_x
$* + H_2O \rightarrow H_2O*$	-0.97	-0.93	-0.93
$H_2O* \rightarrow OH* + H^+ + e^-$	0.68	0.57	0.52
$OH* \rightarrow O* + H^+ + e^-$	0.87	0.88	0.86
$O* + H_2O \rightarrow O*(O_v\text{-}H_2O)$	-1.09	-1.36	-1.17
$O*(O_v\text{-}H_2O) + H_2O \rightarrow OOH*(O_v\text{-}H_2O) + H^+ + e^-$	1.33	1.25	1.24
$OOH*(O_v\text{-}H_2O) \rightarrow H_2O* + O_2 + H^+ + e^-$	-2.52	-1.99	-1.98

References:

1. S. Laha, Y. Lee, F. Podjaski, D. Weber, V. Duppel, L. M. Schoop, F. Pielnhofer, C. Scheurer, K. Müller, U. Starke, K. Reuter and B. V. Lotsch, Adv. Energy Mater., 2019, **9**, 1803795.
2. L. J. Zhang, H. Jang, H. H. Liu, M. G. Kim, D. J. Yang, S. G. Liu, X. E. Liu and J. Cho, Angew. Chem. Int. Ed., 2021, **60**, 18821-18829.
3. Y. C. Yao, S. L. Hu, W. X. Chen, Z. Q. Huang, W. C. Wei, T. Yao, R. R. Liu, K. T. Zang, X. Q. Wang, G. Wu, W. J. Yuan, T. W. Yuan, B. Q. Zhu, W. Liu, Z. J. Li, D. S. He, Z. G. Xue, Y. Wang, X. S. Zheng, J. C. Dong, C. R. Chang, Y. X. Chen, X. Hong, J. Luo, S. Q. Wei, W. X. Li, P. Strasser, Y. E. Wu and Y. D. Li, Nat. Catal., 2019, **2**, 304-313.
4. J. Q. Shan, T. Ling, K. Davey, Y. Zheng and S. Z. Qiao, Adv. Mater., 2019, **31**, 1900510.
5. D. Chen, T. T. Liu, P. Y. Wang, J. H. Zhao, C. T. Zhang, R. L. Cheng, W. Q. Li, P. X. Ji, Z. H. Pu and S. C. Mu, ACS Energy Lett., 2020, **5**, 2909-2915.
6. J. Y. Xu, J. J. Li, Z. Lian, A. Araujo, Y. Li, B. Wei, Z. P. Yu, O. Bondarchuk, I. Amorim, V. Tileli, B. Li and L. F. Liu, ACS Catal., 2021, **11**, 3402-3413.
7. J. Q. Shan, C. X. Guo, Y. H. Zhu, S. M. Chen, L. Song, M. Jaroniec, Y. Zheng and S. Z. Qiao, Chem, 2019, **5**, 445-459.
8. J. W. Su, R. X. Ge, K. M. Jiang, Y. Dong, F. Hao, Z. Q. Tian, G. X. Chen and L. Chen, Adv. Mater., 2018, **30**, 1801351.
9. N. Zhang, C. Wang, J. W. Chen, C. Y. Hu, J. Ma, X. Deng, B. C. Qiu, L. J. Cai, Y. J. Xiong and Y. Chai, ACS Nano, 2021, **15**, 8537-8548.
10. J. W. Zhu, Y. Guo, F. Liu, H. W. Xu, L. Gong, W. J. Shi, D. Chen, P. Y. Wang, Y. Yang, C. T. Zhang, J. S. Wu, J. H. Luo and S. C. Mu, Angew. Chem. Int. Ed., 2021, **60**, 12328-12334.
11. D. Chen, R. H. Yu, D. L. Wu, H. Y. Zhao, P. Y. Wang, J. W. Zhu, P. X. Ji, Z. H. Pu, L. Chen, J. Yu and S. C. Mu, Nano Energy, 2022, **100**, 107445.
12. S. C. Sun, H. Jiang, Z. Y. Chen, Q. Chen, M. Y. Ma, L. Zhen, B. Song and C. Y. Xu, Angew. Chem. Int. Ed., 2022, **61**, e202202519.
13. Y. Wu, R. Yao, Q. Zhao, J. P. Li and G. Liu, Chem. Eng. J., 2022, **439**, 135699.
14. L. A. Chong, J. G. Wen, E. R. Song, Z. Z. Yang, I. D. Bloom and W. J. Ding, Adv. Energy Mater., 2023, **13**, 2302306.
15. D. Galyamin, J. Torrero, I. Rodríguez, M. J. Kolb, P. Ferrer, L. Pascual, M. A. Salam, D. Gianolio, V. Celorrio, M. Mokhtar, D. G. Sanchez, A. S. Gago, K. A. Friedrich, M. A. Peña, J. A. Alonso, F. Calle-Vallejo, M. Retuerto and S. Rojas, Nat. Commun., 2023, **14**, 2010.
16. K. Huang, C. L. Lin, G. Q. Yu, P. Du, X. Y. Xie, X. He, Z. C. Zheng, N. Sun, H. L. Tang, X. B. Li, M. Lei and H. Wu, Adv. Funct. Mater., 2023, **33**, 2211102.
17. L. Q. Hou, Z. J. Li, H. Jang, Y. Wang, X. M. Cui, X. M. Gu, M. G. Kim, L. G. Feng, S. G. Liu and X. Liu, Adv. Energy Mater., 2023, **13**, 2300177.
18. J. Wang, L. L. Han, B. L. Huang, Q. Shao, H. L. L. Xin and X. Q. Huang, Nat. Commun., 2019, **10**, 5692.
19. J. Wang, C. Cheng, Q. Yuan, H. Yang, F. Q. Meng, Q. H. Zhang, L. Gu, J. L. Cao, L. G. Li, S. C. Haw, Q. Shao, L. Zhang, T. Cheng, F. Jiao and X. Q. Huang, Chem, 2022, **8**, 1673-1687.
20. Z. P. Shi, J. Li, Y. B. Wang, S. W. Liu, J. B. Zhu, J. H. Yang, X. Wang, J. Ni, Z. Jiang, L. J. Zhang, Y. Wang, C. P. Liu, W. Xing and J. J. Ge, Nat. Commun., 2023, **14**, 843.
21. J. Q. Wang, C. Xi, M. Wang, L. Shang, J. Mao, C. K. Dong, H. Liu, S. A. Kulinich and X. W. Du, ACS Catal., 2020, **10**, 12575-12581.
22. X. J. Cui, P. J. Ren, C. Ma, J. Zhao, R. X. Chen, S. M. Chen, N. P. Rajan, H. B. Li, L. Yu, Z. Q. Tian and D. H. Deng, Adv. Mater., 2020, **32**, 1908126.
23. Z. Li, S. Wang, Y. Y. Tian, B. H. Li, H. J. Yan, S. Zhang, Z. M. Liu, Q. J. Zhang, Y. C. Lin and L. Chen, Chem. Commun., 2020, **56**, 1749-1752.
24. Y. Y. Tian, S. Wang, E. Velasco, Y. P. Yang, L. J. Cao, L. J. Zhang, X. Li, Y. C. Lin, Q. J. Zhang and L. Chen, Iscience, 2020, **23**, 100756.

25. M. Chen, Z. H. Fan, L. H. Ai and J. Jiang, Appl. Surf. Sci., 2021, **564**, 150478.
26. I. G. Kim, A. Lim, J. H. Jang, K. Y. Lee, I. W. Nah and S. Park, J. Power Sources, 2021, **501**, 230002.
27. L. An, F. Yang, C. H. Fu, X. Y. Cai, S. Y. Shen, G. F. Xia, J. Li, Y. Z. Du, L. X. Luo and J. L. Zhang, Adv. Funct. Mater., 2022, **32**, 2200131.
28. C. L. Rong, X. J. Shen, Y. Wang, L. Thomsen, T. W. Zhao, Y. B. Li, X. Y. Lu, R. Amal and C. Zhao, Adv. Mater., 2022, **34**, 2110103.
29. C. Lin, J. L. Li, X. P. Li, S. Yang, W. Luo, Y. J. Zhang, S. H. Kim, D. H. Kim, S. S. Shinde, Y. F. Li, Z. P. Liu, Z. Jiang and J. H. Lee, Nat. Catal., 2021, **4**, 1012-1023.
30. K. X. Wang, Y. L. Wang, B. Yang, Z. J. Li, X. T. Qin, Q. H. Zhang, L. C. Lei, M. Qiu, G. Wu and Y. Hou, Energy Environ. Sci., 2022, **15**, 2356-2365.
31. S. Chen, C. L. Wang, F. Y. Gao, Y. Yang, M. X. Huang, H. G. Tong, Z. Y. Cheng, P. C. Wang, P. C. Wang, J. W. Tu, X. H. Zeng and Q. W. Chen, J. Mater. Chem. A, 2022, **10**, 3722-3731.
32. Y. Z. Wen, C. Liu, R. Huang, H. Zhang, X. B. Li, F. P. G. de Arquer, Z. Liu, Y. Y. Li and B. Zhang, Nat. Commun., 2022, **13**, 4871.
33. Q. L. Wu, K. Jiang, J. H. Han, D. C. Chen, M. Luo, J. Lan, M. Peng and Y. W. Tan, Sci. China Mater., 2022, **65**, 1262-1268.
34. T. T. Wang, Z. J. Li, H. Jang, M. G. Kim, Q. Qin and X. Liu, ACS Sustainable Chem. Eng., 2023, **11**, 5155-5163.
35. Z. X. Wu, Y. L. Wang, D. Z. Liu, B. W. Zhou, P. F. Yang, R. Z. Liu, W. P. Xiao, T. Y. Ma, J. S. Wang and L. Wang, Adv. Funct. Mater., 2023, **33**, 2307010.
36. L. Li, G. W. Zhang, J. W. Xu, H. J. He, B. Wang, Z. M. Yang and S. C. Yang, Adv. Funct. Mater., 2023, **33**, 2213304.
37. Z. Q. Niu, Z. K. Lu, Z. L. Qiao, S. T. Wang, X. H. Cao, X. D. Chen, J. M. Y. Yun, L. R. Zheng and D. P. Cao, Adv. Mater., 2024, **36**, 2310690.
38. L. M. Deng, S. F. Hung, Z. Y. Lin, Y. Zhang, C. C. Zhang, Y. X. Hao, S. Y. Liu, C. H. Kuo, H. Y. Chen, J. Peng, J. Z. Wang and S. J. Peng, Adv. Mater., 2023, **35**, 2305939.
39. T. L. Feng, J. K. Yu, D. Yue, H. Q. Song, S. Y. Tao, G. I. N. Waterhouse, S. Y. Lu and B. Yang, Appl. Catal. B-Environ., 2023, **328**, 122546.
40. Y. Wu, R. Yao, K. Y. Zhang, Q. Zhao, J. P. Li and G. Liu, Chem. Eng. J., 2024, **479**, 147939.
41. N. Yao, H. N. Jia, J. Zhu, Z. P. Shi, H. J. Cong, J. J. Ge and W. Luo, Chem, 2023, **9**, 1882-1896.
42. L. Q. Wu, Q. Liang, J. Y. Zhao, J. Zhu, H. N. Jia, W. Zhang, P. Cai and W. Luo, Chinese J. Catal., 2023, **55**, 182-190.
43. W. J. Zhu, F. Yao, K. J. Cheng, M. T. Zhao, C. J. Yang, C. L. Dong, Q. M. Hong, Q. Jiang, Z. C. Wang and H. F. Liang, J. Am. Chem. Soc., 2023, **145**, 17995-18006.
44. H. Liu, Z. Zhang, J. J. Fang, M. X. Li, M. G. Sendeku, X. Wang, H. Y. Wu, Y. P. Li, J. J. Ge, Z. B. Zhuang, D. J. Zhou, Y. Kuang and X. M. Sun, Joule, 2023, **7**, 558-573.
45. D. F. Zhang, M. N. Li, X. Yong, H. Q. Song, G. I. N. Waterhouse, Y. F. Yi, B. J. Xue, D. L. Zhang, B. Z. Liu and S. Y. Lu, Nat. Commun., 2023, **14**, 2517.
46. H. Y. Jin, X. Y. Liu, P. F. An, C. Tang, H. M. Yu, Q. H. Zhang, H. J. Peng, L. Gu, Y. Zheng, T. S. Song, K. Davey, U. Paik, J. C. Dong and S. Z. Qiao, Nat. Commun., 2023, **14**, 354.
47. Y. Qin, T. T. Yu, S. H. Deng, X. Y. Zhou, D. M. Lin, Q. Zhang, Z. Y. Jin, D. F. Zhang, Y. B. He, H. J. Qiu, L. H. He, F. Y. Kang, K. K. Li and T. Y. Zhang, Nat. Commun., 2022, **13**, 3784.
48. G. Zhou, P. F. Wang, B. Hu, X. Y. Shen, C. C. Liu, W. X. Tao, P. L. Huang and L. Z. Liu, Nat. Commun., 2022, **13**, 4106.
49. L. X. Zhou, Y. F. Shao, F. Yin, J. Li, F. Y. Kang and R. T. Lv, Nat. Commun., 2023, **14**, 7644.
50. Z. Y. Wu, F. Y. Chen, B. Lie, S. W. Yu, Y. Z. Finfrock, D. M. Meira, Q. Q. Yan, P. Zhu, M. X. Chen, T. W. Song, Z. Yin, H. W. Liang, S. Zhang, G. Wang and H. Wang, Nat. Mater., 2023, **22**, 100-108.
51. X. Han, M. Y. Jin, T. T. Chen, T. Chou, J. D. Chen, S. Wang, Y. Yang, J. Wang and H. L. Jin, ACS Mater. Lett., 2024, **6**, 748-755.
52. J. H. Chen, Y. R. Ma, T. Huang, T. L. Jiang, S. Park, J. W. Xu, X. Y. Wang, Q. Peng, S. Liu, G. M. Wang and W. Chen, Adv. Mater., 2024, **36**, 2312369.

53. G. Q. Zhao, W. Guo, M. M. Shan, Y. Y. Fang, G. M. Wang, M. X. Gao, Y. F. Liu, H. G. Pan and W. P. Sun, Adv. Mater., 2024, **36**, 2404213.
54. J. J. Zhang, L. L. Xu, X. X. Yang, S. Guo, Y. F. Zhang, Y. Zhao, G. Wu and G. Li, Angew. Chem. Int. Ed., 2024, **63**, e202405641.
55. W. D. He, X. H. Tan, Y. Y. Guo, Y. H. Xiao, H. Cui and C. X. Wang, Angew. Chem. Int. Ed., 2024, **136**, e202405798.
56. Y. M. Xu, Z. X. Mao, J. F. Zhang, J. P. Ji, Y. Zou, M. Y. Dong, B. Fu, M. Q. Hu, K. D. Zhang, Z. Y. Chen, S. Chen, H. J. Yin, P. R. Liu and H. J. Zhao, Angew. Chem. Int. Ed., 2024, **63**, e202316029.
57. X. Long, B. Zhao, Q. Q. Zhao, X. X. Wu, M. N. Zhu, R. F. Feng, M. Shakouri, Y. Zhang, X. X. Xiao, J. J. Zhang, X. Z. Fu and J. L. Luo, Appl. Catal. B-Environ., 2024, **343**, 123559.
58. L. An, X. Y. Cai, F. Yang, J. B. You, S. Yuan, L. T. Zhao, C. F. Zhao, L. X. Luo, X. H. Yan, S. Y. Shen and J. L. Zhang, Appl. Surf. Sci., 2024, **652**, 159251.
59. D. Chen, R. H. Yu, K. S. Yu, R. H. Lu, H. Y. Zhao, J. X. Jiao, Y. T. Yao, J. W. Zhu, J. S. Wu and S. C. Mu, Nat. Commun., 2024, **15**, 3928.
60. X. Y. Ping, Y. D. Liu, L. X. Zheng, Y. Song, L. Guo, S. G. Chen and Z. D. Wei, Nat. Commun. , 2024, **15**, 2501.